Geoscience Canada
Journal of the Geological Association of Canada
Journal de l'Association Géologique du Canada

Structural Features of the Central Labrador Trough: A Model for Strain Partitioning, Differential Exhumation and Late Normal Faulting in a Thrust Wedge under Oblique Shortening

Elena Konstantinovskaya, Gennady Ivanov, Jean-Louis Feybesse et Jean-Luc Lescuyer

Volume 46, numéro 1, 2019

URI : https://id.erudit.org/iderudit/1059899ar
DOI : https://doi.org/10.12789/geocanj.2019.46.143

Aller au sommaire du numéro

Éditeur(s)

The Geological Association of Canada

ISSN

0315-0941 (imprimé)
1911-4850 (numérique)

Découvrir la revue

Citer cet article

Konstantinovskaya, E., Ivanov, G., Feybesse, J.-L. & Lescuyer, J.-L. (2019). Structural Features of the Central Labrador Trough: A Model for Strain Partitioning, Differential Exhumation and Late Normal Faulting in a Thrust Wedge under Oblique Shortening. *Geoscience Canada*, *46*(1), 5–30. https://doi.org/10.12789/geocanj.2019.46.143

Résumé de l'article

La partie centrale de la ceinture de plissement et de chevauchement de la Fosse du Labrador de vergence vers l'ouest fait partie intégrante de l'Orogène du Nouveau-Québec, et résulte de la collision oblique avec transpression dextre entre le craton Supérieur archéen et le bloc archéen de la Zone noyau pendant l'Orogenèse trans-hudsonienne (1.82–1.77 Ga). Les structures associées à la transpression dextre sont bien établies dans la partie nord de l'orogène mais pas dans la partie centrale. Nous présentons de nouvelles observations structurales de terrain le long de la traverse ouest–est Minowean-Romanet d'environ 70 km de long, qui comprennent non seulement des évidences de tectonique de chevauchement, mais également des exemples encore non documentés de zones de cisaillement ductile et de structures d'extension fragiles, demi-fragiles et ductiles à la fois dans les parties frontales et arrière du prisme d'accrétion tectonique. La linéation minérale à faible plongement récemment décrite, les axes de plis cylindriques et les zones de cisaillement mylonitique dextre dans le compartiment inférieur de la faille de Romanet sont subparallèles à l'orogène et reflètent une phase précoce de la convergence oblique. La linéation et les stries minérales sur les plans des failles normales dans le compartiment supérieur de la faille de Romanet sont orientées orthogonalement à l'orogène et correspondent à la phase ultérieure d'exhumation induite par les effets combinés de l'érosion et de l'accrétion basale. Pour expliquer l'augmentation du degré d'exhumation le long de l'orogène du nord-ouest au sud-est dans la zone d'étude, nous proposons un modèle de partitionnement de la déformation et de l'exhumation différentielle résultant des variations longitudinales du raccourcissement et de l'érosion dans un contexte de convergence oblique.

ANDREW HYNES SERIES: TECTONIC PROCESSES

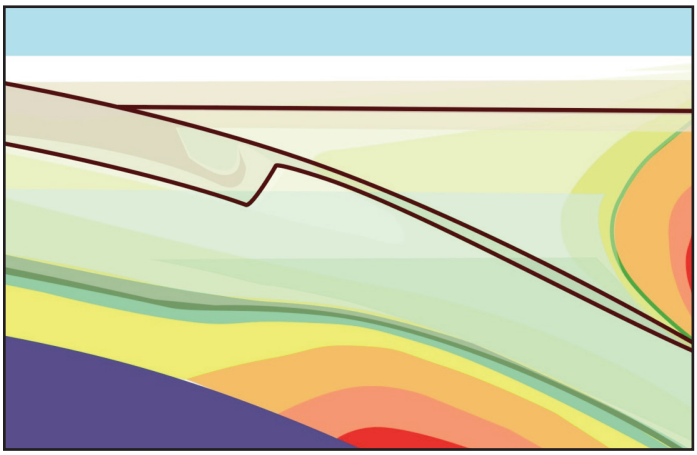

Structural Features of the Central Labrador Trough: A Model for Strain Partitioning, Differential Exhumation and Late Normal Faulting in a Thrust Wedge under Oblique Shortening

E. Konstantinovskaya[1], G. Ivanov[2,3], J.L. Feybesse[3,4] and J.L. Lescuyer[3]

[1]University of Alberta, Earth and Atmospheric Sciences
1-26 Earth Sciences Building, Edmonton, Alberta,
T6G 2E3, Canada
E-mail: konstant@ualberta.ca

[2]IOS Services Geoscientifiques Inc.
1319 Boulevard Saint-Paul, Chicoutimi, Quebec, G7J 3Y2, Canada

[3]senior consulting geologist, formerly with Areva (presently Orano),
Tour Areva , 1 place Jean Millier, 92084 Paris, France

[4]Deceased

SUMMARY

The west-verging fold and thrust belt of the Central Labrador Trough originated as a part of the New Quebec Orogen from rift inversion as a result of oblique collision and dextral transpression between the Archean Superior craton and the Archean block of the Core Zone during the Trans-Hudson orogeny (1.82–1.77 Ga). The structures associated with dextral transpression are well established in the northern segment of the orogen but not in the central part. We present new field structural observations along the ca. 70 km long W–E Minowean-Romanet transect that include not only elements of thrust tectonics but also previously undocumented examples of strike-slip shear zones and late brittle, semi-brittle and ductile extensional structures which occurred both in the frontal and rear parts of the thrust wedge. The newly described low-angle mineral lineation, axes of cylindrical folds and dextral mylonitic shear zones in the footwall of the Romanet Fault are oriented subparallel to the orogen and reflect the early phase of oblique convergence. Mineral lineations and striations on planes of normal faults in the hanging wall of the Romanet Fault are oriented orthogonal to the orogen and correspond to a later phase of exhumation driven by the combined effects of erosion and underplating. To explain the increase in the degree of exhumation along the orogen in the study area from NW to SE, we propose a model of strain partitioning and differential exhumation that resulted from longitudinal variations of shortening and erosion under an oblique convergence setting.

RÉSUMÉ

La partie centrale de la ceinture de plissement et de chevauchement de la Fosse du Labrador de vergence vers l'ouest fait partie intégrante de l'Orogène du Nouveau-Québec, et résulte de la collision oblique avec transpression dextre entre le craton Supérieur archéen et le bloc archéen de la Zone noyau pendant l'Orogenèse trans-hudsonienne (1.82–1.77 Ga). Les structures associées à la transpression dextre sont bien établies dans la partie nord de l'orogène mais pas dans la partie centrale. Nous présentons de nouvelles observations structurales de terrain le long de la traverse ouest–est Minowean-Romanet d'environ 70 km de long, qui comprennent non seulement des évidences de tectonique de chevauchement, mais également des exemples encore non documentés de zones de cisaillement ductile et de structures d'extension fragiles, demi-fragiles et ductiles à la fois dans les parties frontales et arrière du prisme d'accrétion tectonique. La linéation minérale à faible plongement récemment décrite, les axes de plis cylindriques et les zones de cisaillement mylonitique dextre dans le compartiment inférieur de la faille de Romanet sont subparallèles à l'orogène et reflètent une

Geoscience Canada, v. 46, http://www.dx.doi.org/10.12789/geocanj.2019.46.143 pages 5–30

GC Data Repository: Andrew Hynes Series: Tectonic Processes at https://GAC.ca/GC-data-repository/.

phase précoce de la convergence oblique. La linéation et les stries minérales sur les plans des failles normales dans le compartiment supérieur de la faille de Romanet sont orientées orthogonalement à l'orogène et correspondent à la phase ultérieure d'exhumation induite par les effets combinés de l'érosion et de l'accrétion basale. Pour expliquer l'augmentation du degré d'exhumation le long de l'orogène du nord-ouest au sud-est dans la zone d'étude, nous proposons un modèle de partitionnement de la déformation et de l'exhumation différentielle résultant des variations longitudinales du raccourcissement et de l'érosion dans un contexte de convergence oblique.

INTRODUCTION

Many collisional orogenic belts developed at oblique convergent plate boundaries are characterized by spatial and temporal distribution of deformation caused by strain partitioning between the two plates. As it has been shown in the south-central Canadian Rockies, the Western Alps, the Variscides of France, and in Taiwan, the regional stretching mineral lineation and axes of cylindrical folds are oriented subparallel to an orogen and were formed in the footwall of a convergent boundary during the earliest phase of deformation and prograde metamorphism as a result of oblique subduction (Ellis 1986; Ellis and Watkinson 1987; Echtler and Malavieille 1990; Matte et al. 1998). The later-formed stretching mineral lineations are oriented transverse to the orogen and occur either at an imbricated hanging wall–footwall transition zone or within the hanging wall. Stretching mineral lineations transverse to the orogen may be associated either with thrust emplacement (Malavieille et al. 1984; Lacassin 1987; Burg et al. 1987) or with normal faulting during the exhumation phase (Ellis 1986; Ellis and Watkinson 1987). Normal faulting may occur in a thrust wedge during shortening and syncollisional exhumation under the combined effect of continuous tectonic underplating (i.e. different decoupling levels acting at different depths within the wedge) and surface erosion (Konstantinovskaia and Malavieille 2005; Malavieille 2010; Konstantinovskaya and Malavieille 2011). On the basis of analog experiments, Malavieille and Konstantinovskaya (2010) have suggested that deep crustal-scale normal shear zones and superimposed brittle normal faults in the uppermost crust may form during compressional tectonics associated with continental subduction.

Longitudinal variation of the amount of shortening along an orogen may too result in strain partitioning in a thrust wedge. This mechanism was suggested for the western Alps where progressively increasing shortening along the orogen is likely associated with changes in the amount of exhumation from the south to the north of the orogen (Rosenberg et al. 2015).

The field structural observations in the Central Labrador Trough presented in this study show that the tectonic evolution of this collisional belt cannot be explained by a two-dimensional model of orogeny but represents an excellent example of strain partitioning and differential exhumation occurring in a thrust wedge during oblique convergence.

The Labrador Trough is a Paleoproterozoic collisional fold and thrust belt of the New Quebec Orogen (NQO) (Fig. 1).

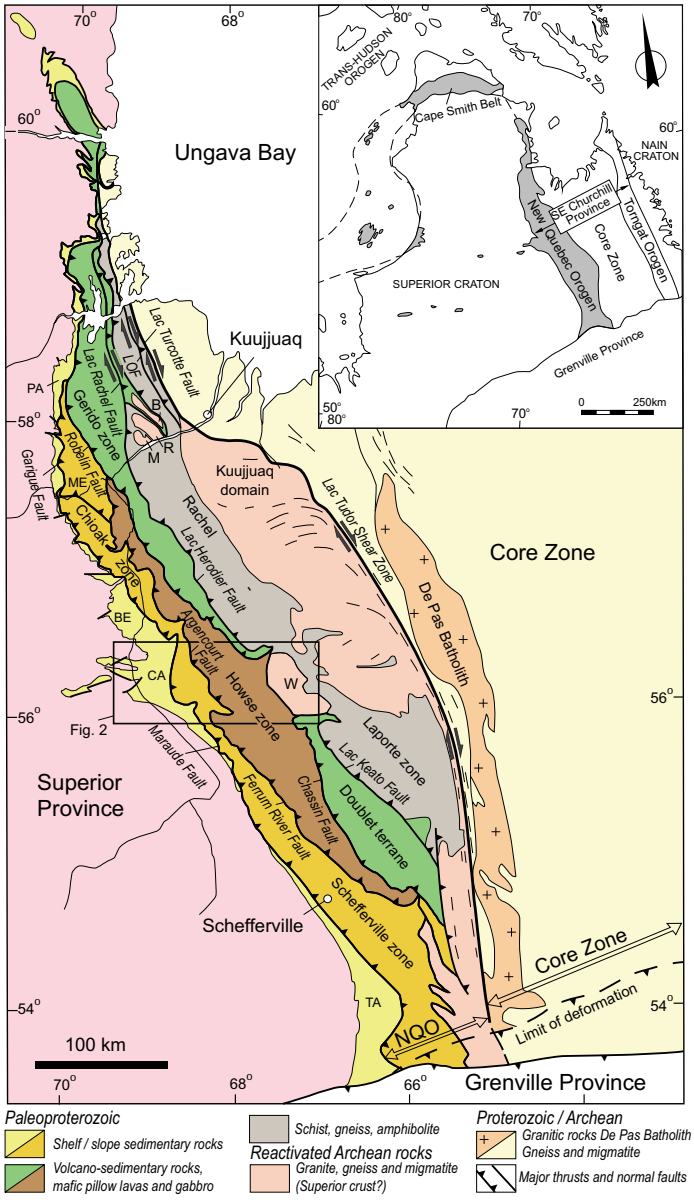

Figure 1. Major tectonic zones of the New Quebec Orogen (NQO) modified after Wardle et al. (2002), Clark and Wares (2004) and Corrigan et al. (2018). BE –Berard, CA –Cambrien, ME –Mélèzes, PA –Payne, TA –Tamarack zones; allochthonous domes of Archean basement gneiss: B –Boulder, M –Moyer, R –Renia, W –Wheeler; *LOF* –Lac Olmstead Fault. The box indicates location of Figure 2a.

The belt extends for about 800 km from the front of the Grenville belt in the south to Ungava Bay in the north. It originated as an incipient rift developed on the eastern margin of the Superior craton in the Paleoproterozoic (Hoffman 1988; Wardle et al. 2002; Clark and Wares 2004). During the rift inversion, voluminous nappes of mafic rocks were thrust over the sedimentary successions of the continental margin of the Superior craton. The rift inversion and formation of the NQO occurred as a result of oblique collision and dextral transpression between the eastern margin of the Archean Superior craton and an Archean block in the Core Zone during the Trans-Hudson orogeny at 1.82–1.77 Ga (Hoffman 1990; Wardle et al. 1990, 2002; Clark and Wares 2004). Strain was partitioned

across the belt between the SW-directed thrusting toward the Superior craton (foreland) and dextral strike-slip faulting in the Rae Province (hinterland) (Hoffman 1990). The dextral component was recognized in some thrust faults, such as Lac Rachel Fault, Lac Olmstead Fault, Lac Turcotte Fault, and Lac Tudor Shear Zone at the rear part in the wedge (Fig. 1), that are considered to accommodate the dextral transpression during the orogeny (Goulet et al. 1987; Girard 1990; Hoffman 1990; Moorhead and Hynes 1990; Goulet 1995; Wardle et al. 2002; Vanier et al. 2017). However, no well-documented ductile strike-slip shear zones that would accommodate strain partitioning during the oblique collision have yet been reported in the Central Labrador Trough between latitudes 56˚15' N and 56˚30' N (Fig. 2a). Neither the tectonic exhumation phase, nor the associated fault kinematics has been thoroughly studied in the region. The brittle normal faults recognized in the eastern part of the orogen (Romanet horst) were interpreted as small-scale displacement faults, referred to late tectonic adjustments (Clark 1986; Clark and Wares 2004). No late brittle or semi-brittle normal faults have been documented in the foreland zone of the orogen at the latitude of the study area.

In this paper, we present new results of structural analysis carried out during detailed field mapping in selected areas along the 70 km W–E Minowean–Romanet transect across the Central Labrador Trough between latitudes 56˚15' N and 56˚30' N (Fig. 2a). New evidence for dextral mylonitic shearing and brittle and semi-brittle normal faulting were documented in the frontal part of the orogen. Low-angle stretching mineral lineations and axes of cylindrical folds oriented parallel to the orogen in a dextral mylonitic shear zone, normal brittle faults and shear zones were observed in the hinterland of the orogen. We propose a model of strain partitioning and differential exhumation associated with longitudinal variations of shortening and erosion under an oblique convergence setting to explain the observed structural features.

GEOLOGICAL BACKGROUND

Stratigraphy

The Paleoproterozoic sedimentary succession of the Central Labrador Trough consists of two distinct depositional cycles (Fig. 2b) separated by an erosional unconformity and a possible episode of tectonic disturbance (Dimroth 1978; Le Gallais and Lavoie 1982; Clark and Wares 2004). During the first sedimentary cycle (2169–2142 Ma), the incipient rift was filled with continental deposits and a platform succession (Seward and Pistolet groups) overlain by basin deposits (Swampy Bay Group) closer to the Superior margin, and relatively deeper water sedimentary rocks, basalt (Bacchus Formation) and voluminous gabbro sills–sediment complexes (Montagnais Group) in the rift area (Le Gallais and Lavoie 1982; Clark and Wares 2004). During the second sedimentary Paleoproterozoic transgressive cycle (1884–1870 Ma), the siliciclastic rocks (Wishart Formation), ferriferous shale, siltstone (Ruth Formation), cherty ironstone (Sokoman Formation) of the Ferriman Group and basin turbidites (Menihek Formation) accumulated (Dimroth 1978; Clark and Wares 2004).

The base of the Paleoproterozoic sedimentary succession (Dimroth 1978) in the Central Labrador Trough, known as the Seward Group, includes fluvial conglomerate and arkosic sandstone of the Chakonipau Formation that are overlain by mudstone, dolomitic sandstone and dolomite of the Portage Formation in the west and by dolomite of the Dunphy Formation in the east (Fig. 2b). To the west, conglomerate and fluvial deposits of the Sakami Formation fill graben and half-graben of the Lac Cambrien rift zone and are correlated to the rocks of the Seward Group (Clark 1984; Hoffman 1988). Further to the east, meta-arkose, metaquartzite, quartz–albite–sericite schist and metamorphosed pebble conglomerate of the Milamar Formation overlie Archean gneiss of the Wheeler dome with an erosional contact (Dimroth 1978). Upwards, the Pistolet Group (PI) is composed of pelitic rocks (mudstone and siltstone) with minor dolomite (Lace Lake Formation), quartz arenite, dolomitic sandstone and dolomite (Alder Formation), and mudstone and siltstone (Uvé Formation). The Pistolet Group is overlain by turbidite mudstone, siltstone and sandstone of the Swampy Bay Group (Hautes-Chutes, Savigny and Otelnuk formations) in the west, and by conglomerate, sandstone and slate of the Du Chambon and Romanet formations in the east. Pillowed and massive basalt with subordinate slate interlayers of the Bacchus Formation overlie the Lace Lake Formation in the eastern part of the region. The platform dolomitic reef complex of the Denault Formation records a marine regression at the end of the first sedimentary cycle.

The age of the basal units of the first cycle of the Paleoproterozoic succession is determined on the basis of a granophyre dyke related to the lac Cramolet gabbro sill, which intruded red beds of the Chakonipau Formation (Seward Group) and has a U–Pb zircon age of 2169 ± 4 Ma (Rohon et al. 1993). A rhyolite dyke cutting through basalt in the upper part of the Bacchus Formation was dated by the U–Pb method at 2142 +4/–2 Ma (T. Krogh and B. Dressler, unpublished data cited by Clark 1984). Thus, the onset of rifting on the continental margin of the Superior craton, emplacement of mafic rocks and accumulation of sedimentary succession of the first cycle started prior to 2169 Ma and mostly ended by 2142 Ma (Wardle et al. 1990; Rohon et al. 1993; Clark and Wares 2004). It was suggested by Clark and Wares (2004) that the end of the first cycle could be extended to 2.06 Ga taking into consideration the heavy carbon isotopic composition ($\delta^{13}C$ ranging from +5 to +15.4‰) of dolomite of the Alder and Uvé formations (Melezhik et al. 1997), typical for carbonate rocks formed between 2.22 and 2.06 Ga (Karhu and Holland 1996).

The Montagnais Group includes gabbro sills and ultramafic rocks of the Labrador Trough, emplaced within stratigraphic units of the first and second sedimentary cycles (Findlay et al. 1995; Clark and Wares 2004). The Montagnais mafic sills that are coeval with the second sedimentary cycle are considered to indicate transitional MORB-like magmatism during renewed rifting on the Superior margin at about 1.88–1.87 Ga (Skulski et al. 1993).

http://www.dx.doi.org/10.12789/geocanj.2019.46.143

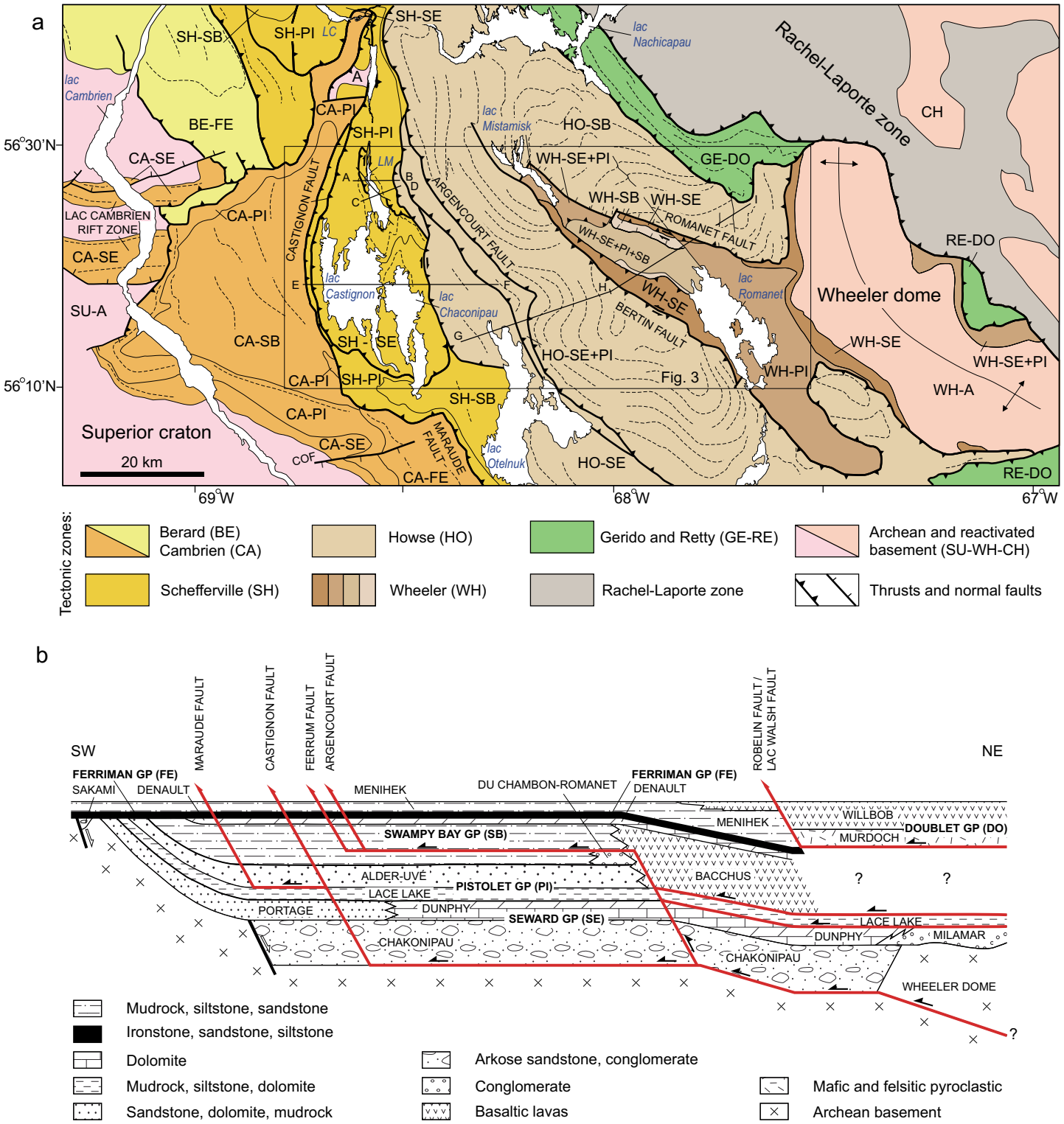

Figure 2. Map of tectonic zones (a) and a generalized pre-thrust reconstruction of Paleoproterozoic sedimentary succession (b) of the Central Labrador Trough, modified after Dimroth (1978), Clark (1986) and Clark and Wares (2004). Tectonic zones: BE –Berard, CA –Cambrien, HO –Howse, SH –Schefferville, WH –Wheeler; SU-WH-CH –Archean (A) rocks of the Superior craton (SU-A) and the Wheeler dome (WH-A) and undivided reactivated Archean rocks of the Southeast Churchill (CH) crustal domain. Stratigraphic groups: DO –Doublet, FE –Ferriman, PI –Pistolet, SB –Swampy Bay, SE –Seward. *COF* –Cambrien-Otelnuk Fault; lac Minowean (*LM*), lac Canichiko (*LC*). The box indicates the location of the study area shown in Figure 3. Solid lines A–B, C–D, E–F, and G–H–I, show the locations of cross-sections in Figures 5 and 6. Dashed lines on the map indicate the structural trend.

The siliciclastic and ferriferous rocks of the Ferriman Group (FE) and basin turbidites of the Menihek Formation of the second sedimentary cycle are present in the western part of the Central Labrador Trough, to the northwest (lac Cambrien) and to the south (the Cambrien-Otelnuk Fault) of the study area (Fig. 2a). The siliciclastic rocks of the Ferriman Group are chrono-stratigraphically correlated with basalt and flysch of the Doublet Group (Fig. 2b) that occur in the eastern part of the orogen (Dimroth 1978; Wardle and Bailey 1981; Le Gallais and Lavoie 1982; Findlay et al. 1995; Clark and Wares 2004). Pyroclastic rocks (tuff and volcanic breccia) of the Murdoch Formation form the base of the Doublet Group are overlain by basalt of the Wilbob Formation east of the Lac Walsh Fault (Fig. 2b), both units being correlated with turbidites of the Menihek Formation (Clark and Wares 2004). The Sokoman Formation in the western part of the orogen is correlated with contemporary intrusive dykes, tuff cones and diatremes of carbonatite and meimechite of the Castignon Complex (Dimroth 1978; Dressler 1979; Chevé 1993; Clark and Wares 2004). The U−Pb age of zircon from a carbonatite dyke of the Castignon complex is 1880 ± 2 Ma (Chevé and Machado 1988). An additional geochronological dataset from the north and south of the NQO referenced in Clark and Wares (2004) indicates the time interval of 1884−1870 Ma for the deposition of the second sedimentary Paleoproterozoic cycle. According to these data, zircon from a glomeroporphyritic gabbro that intruded the Hellancourt Formation gave a U−Pb age of 1874 ± 3 Ma and from rhyodacite in the upper Murdoch Formation yielded an identical U−Pb age of 1870 ± 4 Ma (Machado et al. 1997).

Both the stratigraphic successions of the first and second cycles are characterized by a classic basinward thickening. Each cycle started with a shelf phase of fluvial and/or platformal lithofacies deposited in an oxidized environment (Seward, Pistolet and Ferriman groups), followed by a basin phase with reduced facies (Swampy Bay Group and Menihek Formation) (Le Gallais and Lavoie 1982; Clark and Wares 2004). The sedimentary rocks of the second cycle unconformably overlie (Dimroth 1978) the succession of the first sedimentary cycle and locally Archean basement. This has been interpreted either as a low-angle erosional unconformity resulting from a slight uplift of the Archean foreland (Dimroth 1978), or as an angular unconformity corresponding to the pre-Wishart (Chevé 1993) or proto-Hudsonian (Le Gallais and Lavoie 1982) deformation stage.

Tectonic Structure

The Labrador Trough (Fig. 1) consists of four principal parautochthonous and allochthonous lithotectonic zones composed of Paleoproterozoic sedimentary and/or volcanic and magmatic rocks: Schefferville, Howse, Gerido-Doublet and Rachel-Laporte (Dimroth 1978; Clark and Wares 2004). In the west, these zones are bound by autochthonous zones of sedimentary cover of the Superior craton (Fig. 1): Tamarack, Berard, Cambrien and Payne. The parautochthonous and allochthonous tectonic zones are delineated by major west-verging NW−SE-striking thrust faults extending over 80 km to 250 km, e.g. the Maraude, Ferrum River, Argencourt, Chassin and Lac Herodier faults (Fig. 1).

In the Central Labrador Trough (Fig. 2a), the autochthonous Cambrien zone and parautochthonous Schefferville zone are composed of Paleoproterozoic sedimentary rocks the Seward, Pistolet and Swampy Bay groups (Fig. 2b) with a variable but limited presence of the Montagnais Group gabbro. The ironstone and sedimentary rocks of the Ferriman Group are preserved in the Berard (BE-FE) zone and Cambrien (CA-FE) zones located to the northwest and to the south of the study area, respectively (Fig. 2a).

The autochthonous Cambrien zone is characterized by two different tectonic styles (Fig. 2a). To the west, Archean gneiss basement of the Superior craton is faulted, and the graben and half-graben of the Lac Cambrien rift zone filled by rocks of the Sakami Formation are delimited by the SW−NE normal faults (Clark 1984; Clark and Wares 2004). Some of these normal faults were reactivated as reverse faults during the Trans-Hudson orogeny. The similar SW−NE-striking Cambrien-Otelnuk normal fault (Fig. 2a) delineates an escarpment in the Archean basement to the south of the study area. The Archean gneiss here is overlain with a basal unconformity by the units of the Portage Formation (the Chakonipau Formation is missing). This escarpment was uplifted during the early stages of Paleoproterozoic sedimentation and represents the source terrain for the Chakonipau Formation, accumulated to the north (Dimroth 1978). To the east of lac Cambrien, the Paleoproterozoic sedimentary succession thickens and is composed of units of the Seward, Pistolet and Swampy Bay groups. These rocks deformed in NW−SE-striking folds with limbs dipping to the NE and SW at 25° to 80° and with steep schistosity dipping to the NE at 55°−75° (Dimroth 1978; Chevé 1993). Thrust faults with minimal displacement (Fig. 2a) are mapped in the rocks of the Ferriman Group in the Berard zone (Dimroth 1978; Clark and Wares 2004).

The parautochthonous Schefferville zone is characterized by imbricate structure mostly defined by NW−SE and N−S-striking folds and SW-verging thrust faults. The SW-verging Maraude and Castignon thrust faults separate the rocks of the Cambrien and Schefferville zones (Fig. 2a). These faults join different detachment levels at depth (Fig. 2b); either within or at the base of Paleoproterozoic sedimentary succession and Archean Wheeler dome (Clark and Wares 2004). The detached crustal block of Archean granite-gneiss basement (A) is exposed within the Schefferville zone (Fig. 2a) to the north of the study area, south of the lac Canichiko (Clark and Wares 2004).

The allochthonous Howse zone is composed of voluminous sills of gabbro (Montagnais Group) and pillows and massive flows of basalt with subordinate sedimentary rocks (Bacchus Formation of the Swampy Bay Group, HO-SB). The thick succession of mafic rocks forms nappes emplaced over the rocks of the Schefferville zone along the Argencourt thrust fault. A detached crustal block of Archean granite-gneiss basement is recognized within the Howse zone in the lac Colombet area located about 50 km to the north of the crustal block in the Schefferville zone (Clark and Wares 2004).

http://www.dx.doi.org/10.12789/geocanj.2019.46.143

The allochthonous Wheeler zone is located in the valley of the lacs Mistamisk and Romanet in the eastern part of the study area (Fig. 2a). The Wheeler zone includes Paleoproterozoic sedimentary rocks of the Seward, Pistolet and Swampy Bay groups and gneiss of Archean basement of the Wheeler dome (Dimroth 1978; Clark and Wares 2004).

The sedimentary units of the Seward (WH-SE), Pistolet (WH-PI) and Swampy Bay (WH-SB) groups of the Wheeler zone are exposed between two nappes of mafic rocks of the Howse zone (Fig. 2a) in a structure known as the Romanet horst delimited by the Bertin and Romanet faults (Le Gallais and Lavoie 1982; Chevé 1985; Clark 1986). These units represent the eastern facies of the sedimentary succession of the Schefferville zone (Le Gallais and Lavoie 1982; Clark and Wares 2004) but are strongly deformed and partially metamorphosed (greenschist facies) and locally contain lenses of the Montagnais gabbro and/or amphibolite and peridotite (Dimroth 1978; Dimroth and Dressler 1978; Clark and Wares 2004). The sedimentary units of the Romanet horst are interpreted as forming an erosional tectonic window below a nappe of mafic rocks of the Howse zone (Dimroth 1978; Clark and Wares 2004). In this study, we propose to rename the Romanet horst to the Romanet antiform in accordance with new data on the kinematics of the bounding faults as explained below.

The Wheeler dome (WH-A) is composed of albite−sericite−biotite gneiss (Fig. 2a) belonging to re-worked Archean basement (Dimroth 1978). A crystallization age of 2668 ± 5 Ma has been recently established for tonalite of the Wheeler dome based on SHRIMP U−Pb geochronological results obtained from zircon (Rayner et al. 2017; Corrigan et al. 2018). In the NE corner of the Wheeler dome, the gneiss has been retrograded to lower amphibolite facies as muscovite−biotite−plagioclase gneiss. Extremely sheared gneiss retrograded to sericite−biotite grade occurs in some zones in the southwest of the dome. According to Dimroth (1978), the Wheeler dome at its southwestern boundary is covered by metamorphosed arkose and arkosic conglomerate of the Milamar Formation (Fig 3) suggesting initially an unfaulted stratigraphic contact between Archean gneiss and Paleoproterozoic sedimentary cover. The Milamar arkosic sandstone and pebble conglomerate, dolomitic sandstone and dolomite are metamorphosed under greenschist facies (quartz−albite−sericite and calcite−epidote−tremolite schist and marble) and strongly deformed displaying undulatory extinction in quartz grains and mylonitic folded schistosity (Dimroth 1978). Clark and Wares (2004) suggested a major decollement is located at the base of the Wheeler dome (Fig. 2b), which implies that the gneissic basement and its sedimentary cover are allochthonous.

The Gerido and Retty zones (GE-RE) in the eastern part of the orogen (Fig. 2a) are composed of pyroclastic and sedimentary rocks with numerous basaltic lava flows (Doublet Group) and sills of mafic and ultramafic rocks of the Montagnais Group. These rocks form a synclinorium overturned to the west and thrust over the succession of the Wheeler zone (Figs. 1, 2) along the Robelin, Lac Walsh and Chassin faults (Clark and Wares 2004).

The hinterland of the Central Labrador Trough is composed of gneiss, migmatite, migmatized metasedimentary schist and amphibolite of the Rachel-Laporte zone (Figs. 1, 2a), grading into reworked Archean basement rocks and granitic plutons of the Kuujjuaq domain further to the east (Hoffman 1988; Wardle et al. 1990, 2002; Charette et al. 2017; Corrigan et al. 2018). The rocks of the Rachel-Laporte zone are thrust over the volcano-sedimentary succession of the Gerido and Retty zones (Wardle and Bailey 1981; Charette et al. 2017; Rayner et al. 2017).

Deformation and metamorphic events occurred in the NQO during the Trans-Hudson orogeny between > 1.87 Ga and 1.77 Ga (Machado et al. 1989; Machado 1990; Perreault and Hynes 1990; Wardle et al. 1990; Machado et al. 1997; Wardle et al. 2002). In the northern sector of the orogen, two metamorphic events related to crustal thickening and deformation occurred in the inner zone during collision at 1.845 Ga (granulite facies) and 1.83 Ga (amphibolite facies) (Perreault and Hynes 1990). In the central and southern segment of the hinterland of the Labrador Trough, deformation started at 1.82 Ga, following emplacement of magmatic arc rocks of the De Pas batholith (Fig. 1) and driven by the collision of Archean terranes to the west and east of the batholith (James and Dunning 2000). Amphibolite-facies metamorphism associated with crustal thickening was followed by cooling at 1775 Ma based on U−Pb ages obtained on zircon, monazite and rutile (Machado et al. 1989; James and Dunning 2000).

METHODS

Structural features of the Schefferville, Howse, and Wheeler lithotectonic zones (Fig. 2a) were studied in the Central Labrador Trough between the latitudes of 56°15' N and 56°30' N. Detailed structural and lithologic mapping were carried out in selected key areas 1−7 along the ca. 70 km long Minowean-Romanet transect (Figs. 3, 4), from the extreme frontal point of the Castignon Fault on the western shore of lac Castignon to the hanging wall of the Romanet Fault at the eastern shore of the Romanet River. Four cross-sections (Figs. 5, 6) were constructed through the studied areas based on our field observations and available geologic maps and reports. Structural elements (bedding, cleavage, schistosity, intersection and mineral lineations, fold axes and fault striations) were analyzed on stereonet plots (Figs. 5, 6) for each structural domain demonstrating regional tectonic zonation. All structural orientations are given according to the right-hand rule. On the basis of structural analysis, the main phases of tectonic deformation were distinguished and new 2D and 3D models of tectonic evolution of the region are proposed.

RESULTS

Schefferville Parautochthonous Zone

The Schefferville parautochthonous zone is about 30 km wide and is limited by the frontal Maraude and Castignon imbricated thrust faults in the WSW and the Argencourt thrust fault in the ENE (Fig. 2a).

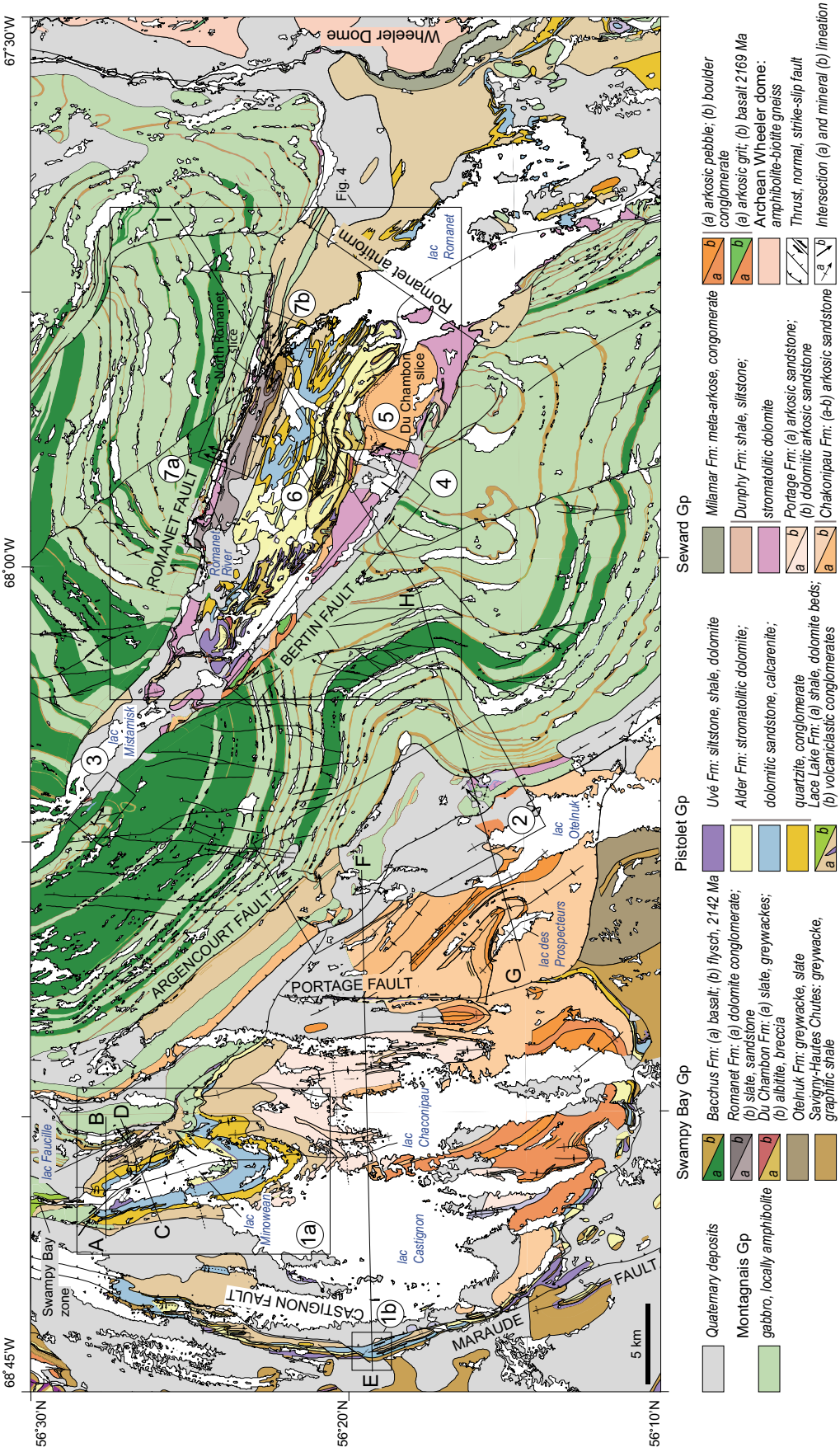

Figure 3. Geological map of the Central Labrador Trough modified after Dimroth (1978) and Clark and Wares (2004). The locations of the cross-sections and areas of structural domains 1–7 used for stereoplots on Figures 5 and 6 are shown.

http://www.dx.doi.org/10.12789/geocanj.2019.46.143

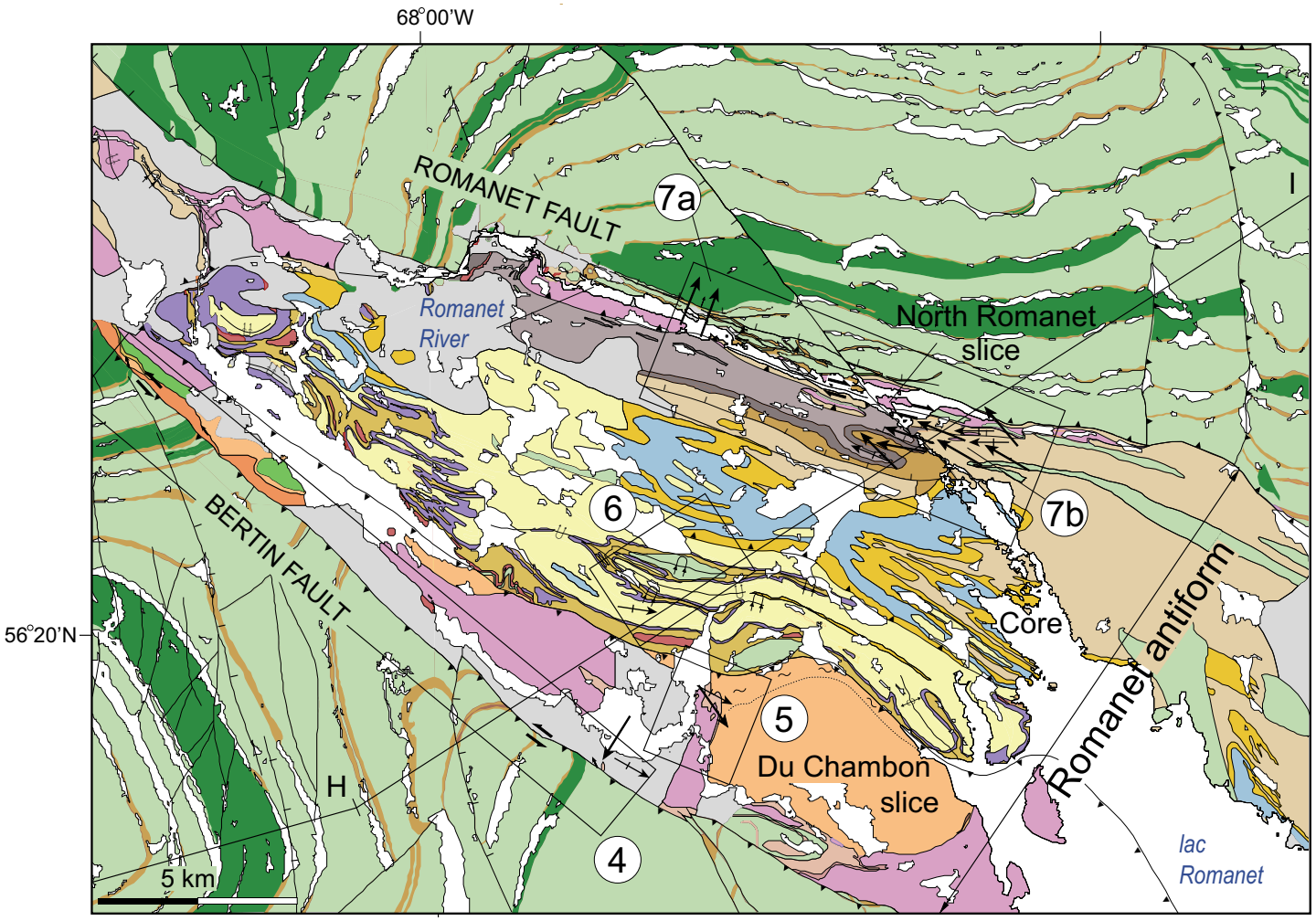

Figure 4. Geological map of the Wheeler zone modified after Dimroth (1978) and Clark and Wares (2004). The locations of cross-section G–H–I and areas of structural domains 4–7 used for stereoplots on Figures 5 and 6 are shown. A coloured legend is shown in Figure 3.

Frontal Thrust Faults

The Maraude Fault extends from north to south for more than 60 km (Fig. 2a). Along this fault, the older parautochthonous units of the Pistolet and Swampy Bay groups were detached along shale of the Lace Lake Formation and thrust to the WSW over the younger autochthonous mudrock of the Hautes Chutes and Savigny formations of the Swampy Bay Group in the west and over the Sokoman Formation of the Ferriman Group in the southwest (Fig. 2b). The more advanced part of the frontal slice is exposed in a 150–200 m high cliff to the west of lac Castignon (Fig. 3, area 1b). Along the cliff, the dolomitic and siliciclastic rocks of the Uvé and Alder formations and pelitic rocks of the Lace Lake Formation are folded in a system of N–S-striking inclined folds verging to the W (Fig. 5, line E–F) and occurring as open synclines (~ 300–400 m wide) and tight anticlines (~ 100–200 m wide). Above the fault contact, the overturned northeastern hanging limb of the frontal inclined syncline dips to the E at about 60° as recognized by the overturned orientation of the stromatolite beds in the limb (Fig. 7a). To the south of lac Castignon, a series of NW–SE-striking overturned synclines and anticlines are mapped along the Maraude Fault, most probably aligned with the fault deviation caused by a lateral (SW–NE) scarp in the basement along the Cambrien-Otelnuk normal fault (Dimroth 1978; Clark and Wares 2004). The apparent westward displacement along the frontal Maraude and Castignon faults is about 20 km as estimated from the geometry of the erosional thrust front on the map (Fig. 2a).

The Castignon Fault extends from north to south for about 35 km along the western shore of lac Castignon (Fig. 3). This fault delineates the parautochthonous Castignon tectonic slice and corresponds to a detachment at the base of the Paleoproterozoic sedimentary succession (Figs. 2b, 5, line E–F). To the E, the tectonic slice is delimited by the Portage Fault (Fig. 3). The apparent westward displacement along the Castignon Fault is about 20 km (Fig. 5, line E–F).

The parautochthonous Castignon tectonic slice is composed of sedimentary rocks of the Seward Group in the south and Pistolet Group in the north (Fig. 3). The oldest red arkosic sandstone and conglomerate of the Seward Group (Chakonipau and Portage formations) form two anticlinoria in the southern part of the slice. The rocks form NNW–SSE-strik-

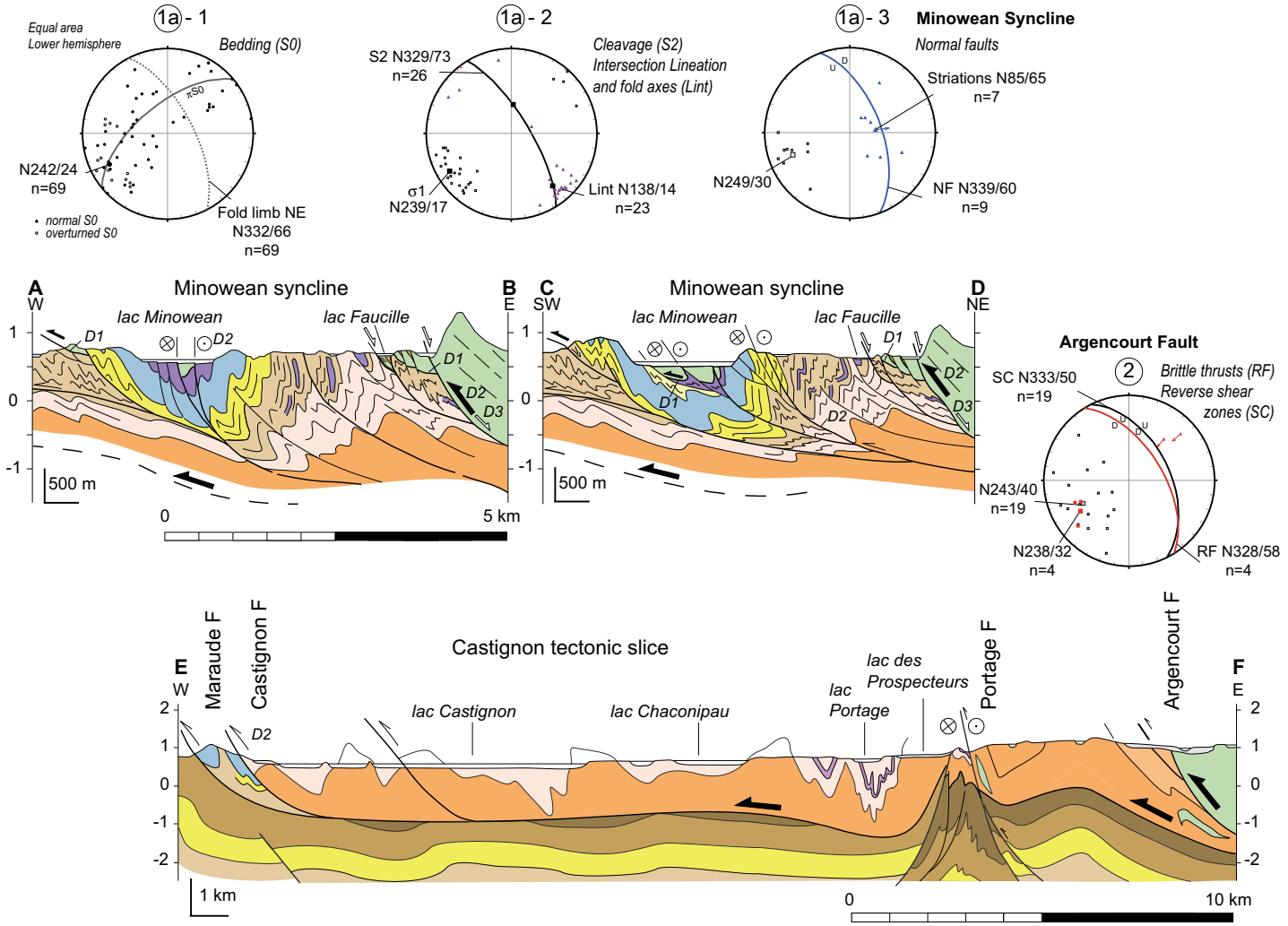

Figure 5. Cross-sections along lines A−B, C−D, and E−F, and stereoplots of principal structural features in studied areas 1−2 along the W−E transect across the Central Labrador Trough. The locations of the cross-sections and coloured legend are shown in Figure 3.

ing, 2−4 km wide open folds, upright in the east and inclined, verging to the WSW, in the frontal part of the slice (Fig. 5, line E−F). The argillaceous, siliciclastic and dolomitic rocks of the Pistolet Group (Lace Lake, Alder, Uvé formations) form the NW−SE-striking Minowean syncline in the north of the slice (Fig. 3, area 1a). The red arkosic sandstone of the Portage Formation (Seward Group) forms the narrow axial zone of a conjugate NW−SE tight anticline to the east of the Minowean fold, in front of the thick Montagnais gabbro frontal slice of the Howse allochthonous zone (Fig. 5, lines A−B, C−D). The inclined folds are verging to the southwest with one of the limbs found in an overturned position.

The Minowean Syncline

The Minowean syncline is about 5 km wide and 15 km long (Fig. 3). The SW-verging fold is steeply inclined: beds of the SW limb dip gently to the NE, while rocks of the NE limb are overturned (Fig. 7b) and dip steeply to the NE at 66°−90° (Fig. 5, stereonet 1a-1). The predominant S2 cleavage is oriented NW−SE (N329/73), parallel to the axial plane (Fig. 5, stereonet 1a-2), and dips at lower angles than bedding in the NE overturned limb (Fig. 7c). The pole of low-angle intersection lineation plunges to the SE (N138/14) and corresponds to the axis of a mesoscopic fold (Fig. 5, stereonet 1a-2). More competent dolomitic sandstone of the Alder Formation is folded in open folds, verging to the SW, second-order synclines that predominantly occur at outcrop scale. The second-order anticlines are rarely observed in outcrops and generally occur as tight cuspate folds in shale of the Uvé and Lace Lake formations. From the analysis of orientations of bedding, cleavage and intersection lineations in the Minowean fold area, the principal compressive stress σ_1 is oriented SW−NE (N239/17) (Fig. 5, stereonet 1a-2).

Fault Sets

Different sets of faults are recognized in the area of the Minowean syncline (Fig. 3). Two sets of the NW−SE-striking thrust faults can be distinguished in the area. D1-phase low-angle thrusts are preserved in the axial zone of the fold and on the eastern and western fold limbs at the contact of gabbro

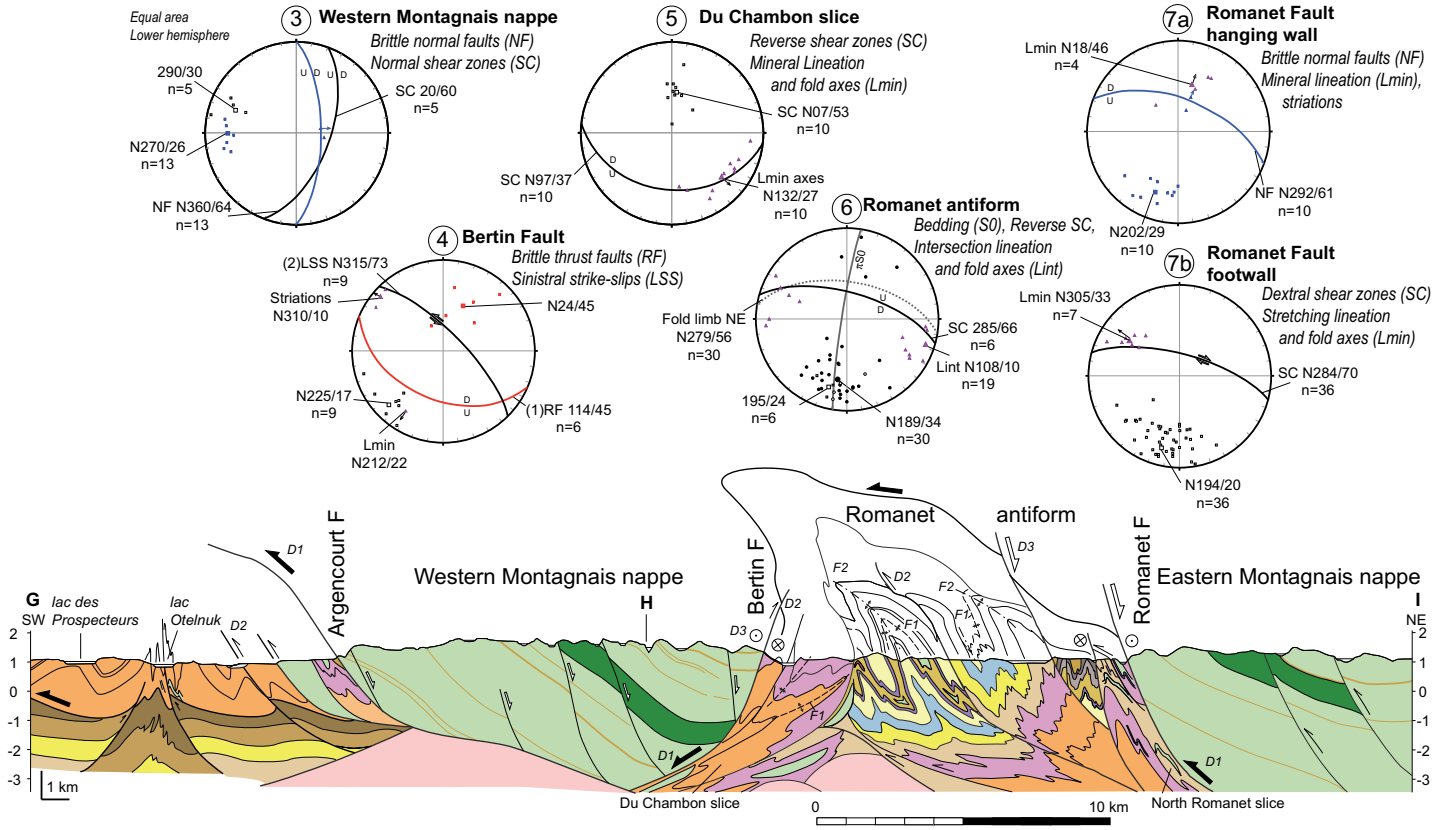

Figure 6. Cross-section along line G–H–I and stereoplots of principal structural features in studied areas 3–7 along the W–E transect across the Central Labrador Trough. The location of the cross-section and colour legend are shown in Figure 3.

slices thrust over shale of the Lace Lake and Uvé formations (Fig. 5, lines A–B, C–D). The D2-phase high-angle thrusts dipping to the northeast mostly affect the northeastern limb. Thrust-related brecciation and boudin rotation (Fig. 7d) were observed in graphitic shale of the Lace Lake Formation below the contact with a gabbro thrust sheet on the western limb of the Minowean fold.

A series of NW–SE right-lateral strike-slip faults with subordinate conjugate left-lateral strike-slip faults (Fig. 7e) and brittle-ductile shear bands of *en echelon* tension fractures affect the northern and northeastern part of the Minowean fold (Fig. 3). These right-lateral strike-slip faults seem to accommodate the dextral displacement along the N–S (N178/80) dextral mylonitic shear zone that runs along the Swampy Bay River at the northern periclinal closure of the Minowean fold (Fig. 3). Along the Swampy Bay dextral mylonitic shear zone, the right-lateral subvertical ductile shear bands SC-C' (Fig. 8a, b) are developed in highly deformed volcaniclastic conglomerate that was previously described as part of the Lace Lake Formation (Brouillette 1989). Pyrite mineralization occurs in the sheared matrix.

Numerous late NNW–SSE-striking near-vertical normal faults (Fig. 7f) of low displacement amplitude (Fig. 5, lines A–B, C–D) cut the NE limb of the Minowean syncline (Fig. 3). The striations on these faults plunge to the ENE with the mean pole oriented N85/65 (Fig. 5, stereonet 1a-3). These faults belong to the same system as the normal faults at the contact between the Montagnais gabbro frontal slice and shale of the Lace Lake Formation to the east of the Minowean syncline (Fig. 3) that are described in the next section.

Howse Allochthonous Zone

The Howse allochthonous zone extends NW–SE for about 300 km and is delimited by the Argencourt and Ferrum River thrust faults to the west and Robelin and Chassin thrust faults to the east (Fig. 1). The Howse zone includes (Fig. 2a): (i) frontal slices composed of sedimentary rocks of the Seward, Pistolet and Swampy Bay groups and gabbro of the Montagnais Group; (ii) two voluminous Montagnais nappes composed of gabbro (Montagnais Group) and basalt with subordinate sedimentary rocks (Bacchus Formation) (Clark and Wares 2004). The two Montagnais nappes are separated by sedimentary rocks exposed in a tectonic window of the Wheeler zone (Fig. 2a).

Frontal Slices of the Howse Zone

An approximately 600 m thick frontal tectonic slice of Montagnais Group gabbro is thrust over the Paleoproterozoic sedimentary succession of the Schefferville zone in the lac Faucille area, to the east of the Minowean syncline (Fig. 3). Below the main steep thrust contact, a series of gabbro lenses are thrust over the Lace Lake Formation shale (Fig. 5, lines A–B, C–D). Late extensional features overprint compressional structures (Fig. 8c, d). The gabbro lenses contain numerous

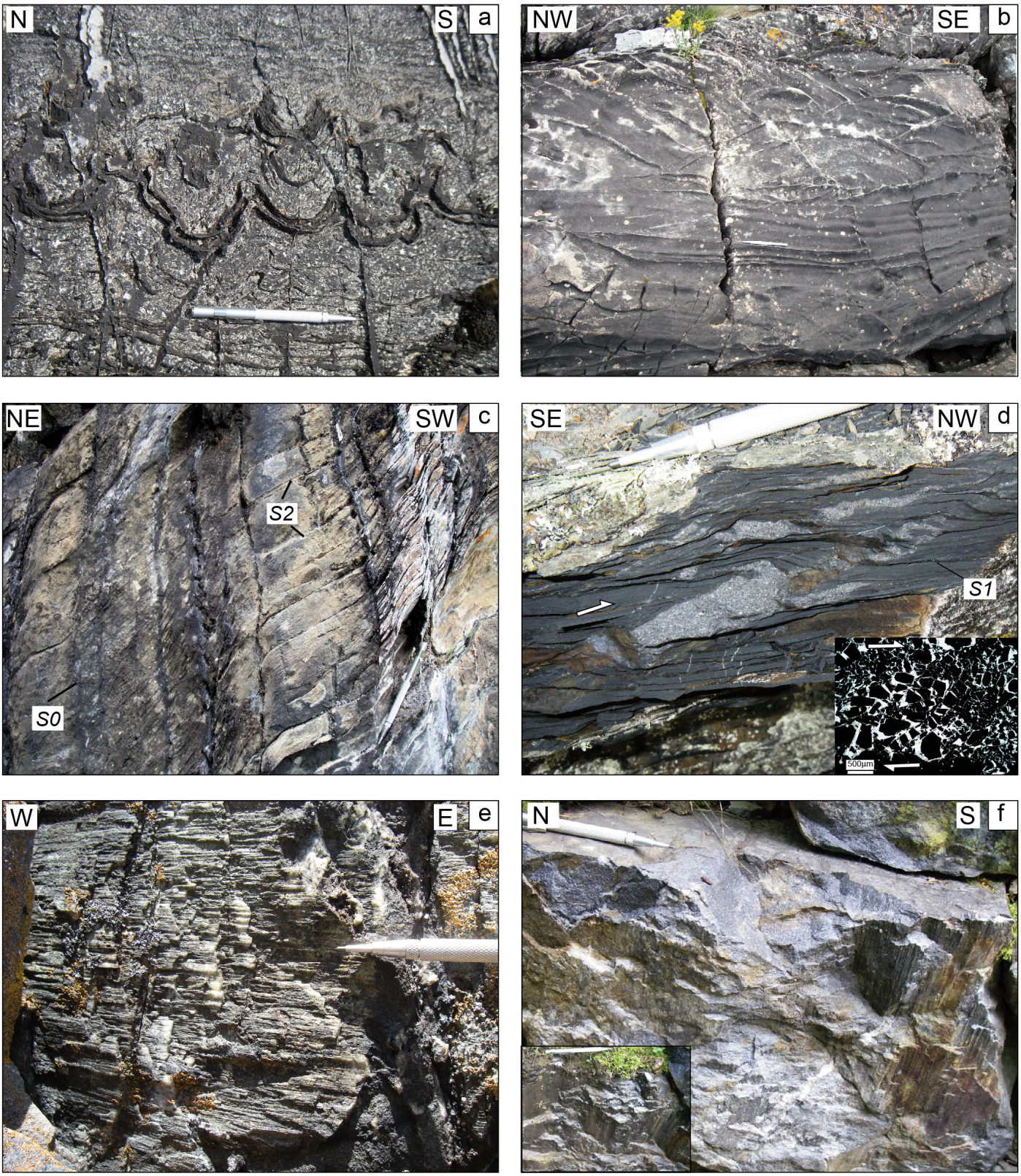

Figure 7. Structural elements of areas of the Schefferville zone (areas 1a and 1b of Figure 3): (a) overturned stromatolite beds in the overturned northeastern limb of a syncline in the hanging wall of the Castignon Fault; (b) overturned cross-bedded stratification in dolomitic quartz sandstone of the Alder Formation, northeastern limb of the Minowean fold; (c) low-angle cleavage and steep bedding dipping to the northeast in the overturned northeastern limb of the Minowean fold; (d) brecciation and boudin rotation in Lace Lake shale below the thrust contact with the Montagnais gabbro in the northwestern part of the Minowean fold; the inset in (d) shows thin section of brecciated graphitic slate from the boudin; (e) striations on a left-lateral strike-slip fault and (f) on normal faults in the northeastern limb of the Minowean syncline.

http://www.dx.doi.org/10.12789/geocanj.2019.46.143

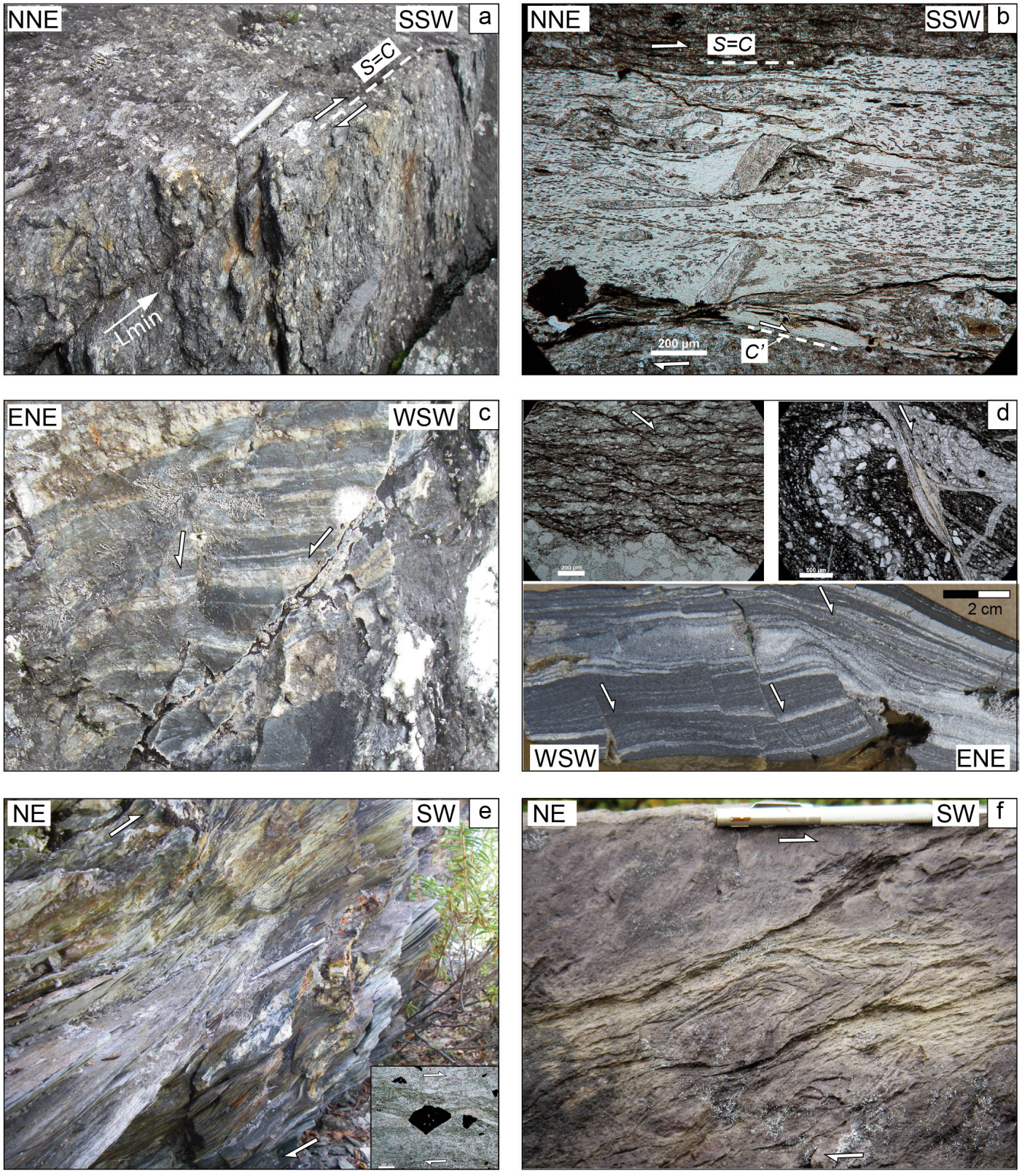

Figure 8. Structural elements of the Schefferville zone (areas 1a and 2 of Figure 3): (a) outcrop and (b) thin-section view of the SC-C' dextral shear bands of the north–south-striking Swampy Bay mylonitic shear zone; (c, d) outcrop, hand specimen and thin sections view of brittle normal faults and semi-brittle normal shear bands in shale of the Lace Lake Formation below the thrust contact with the frontal gabbro tectonic slice at the northeastern limb of the Minowean syncline; (e, f) outcrop views of reverse sheared gabbro of the Montagnais Group in the hanging wall (e) and siltstone of the Lace Lake Formation in the footwall (f) of the Argencourt Fault. The inset in (e) shows stress shadows around a pyrite rotation structure in metasandstone of the Bacchus Formation at the main thrust contact.

steep planes of normal faults with striations dipping to the northeast. Listric normal faults (Fig. 8c), brittle fractures and ductile-brittle shear zones with normal displacement (Fig. 8d) occur in the Lace Lake shale below the contact with massive gabbro. The mean plane of the normal faults (Fig. 5, stereonet 1a-3) is oriented striking NNW–SSE (N339/60) with mean striation plunging ENE (N85/65) indicating a WSW–ENE orientation of late extension.

The Portage Fault delineates the western limit of the frontal slice (Fig. 3), which is mostly composed of red conglomerate and arkosic sandstone of the Chakonipau Formation of the Seward Group (Dimroth 1978). It represents a N–S high-angle thrust fault with a right-lateral strike-slip component that dips steeply (N335/72) to the E (Fig. 5, line E–F). Lenses and sills of gabbro of the Montagnais Group recognized in the sedimentary rocks of the Chakonipau Formation in the eastern part of the slice are considered as *in situ* (Dimroth 1978). The sedimentary rocks in the slice are folded in a series of ca. 1–2 km wide NW–SE open upright synclines and anticlines (Fig. 3). The pole to the NE limb of the mesoscopic fold is oriented N231/12. The high-angle NW–SE schistosity S2 dips to the NE (N326/70). The pole of schistosity corresponds to σ_1 oriented NE–SW (N236/20).

Argencourt Fault

The Argencourt Fault corresponds to a NW–SE regional thrust fault verging to the SW (Figs. 2a, 3) that delineates the western limit of the nappes composed of voluminous gabbro of the Montagnais Group, and basalt and metasedimentary rocks of the Bacchus Formation in the Howse zone (Dimroth 1978; Clark 1986; Clark and Wares 2004). The main thrust contact at the base of the Western Montagnais nappe is localized in metasandstone beds of the Bacchus Formation below the gabbro (Fig. 6, line G–H). The NW–SE reverse SC shear bands (N333/50) dipping to the northeast with mineral lineations plunging to the NE (N40/37) occur in the Bacchus metasandstone (Fig. 5, area 2). The steep S planes in SC shear bands, underlined by oriented mica and fibrous quartz–feldspar–chlorite in oriented pressure shadows around the pyrite grains (Fig. 8e, inset), indicate a reverse sense of displacement and tectonic transport to the SW (N243). The gabbro above the thrust is sheared and transformed into carbonate–chlorite schist (Fig. 8e) characterized by SC reverse shear bands with foliation defined by preferred orientation of chlorite fibers.

Along the frontal part of the Western Montagnais nappe, in the footwall of the Argencourt Fault, relatively thin bodies of strongly sheared gabbro form southwest-verging tectonic lenses in the sedimentary rocks of the Seward and Pistolet groups. Siltstone and sandstone of the Lace Lake Formation and stromatolite dolomite of the Dunphy Formation in the footwall of the Argencourt Fault are characterized by bedding dipping NNE at 35–60° (N290–305/32–58, mean S0 N298/31) and display a strong NW–SE S2 schistosity (Fig. 8f) dipping to the NE (N333/50).

Montagnais Gabbro-basalt Nappes

The gabbro-basalt rocks of the Howse zone form voluminous nappes extending NW–SE for about 300 km (Fig. 2a). A single nappe of mafic rocks, about 30 km wide, in the NW is split southeastwards into two ca. 10 to 20 km wide nappes (Fig. 3), which we name the Western and Eastern Montagnais nappes (Fig. 6, line G–H–I). In the study area, the Western Montagnais nappe is thrust over the sedimentary succession of the Schefferville parautochthonous zone and frontal slices of the Howse zone along the NW–SE Argencourt Fault. In the NE, volcanic and sedimentary rocks of the Gerido zone are thrust to the southwest over the Eastern Montagnais nappe along the NW–SE Robelin thrust fault (Fig. 2a). The Western and Eastern Montagnais nappes are separated by highly deformed sedimentary rocks of the Seward, Pistolet and Swampy Bay groups of the Wheeler zone (Fig. 3) described below as the Romanet antiform and delineated by the NW–SE Bertin and Romanet faults.

The Montagnais nappes are composed of a thick (likely ~ 3–5 km) stratified succession of intercalated Montagnais gabbro sills, Bacchus basalt and relatively thin (a few metres) packages of sedimentary rocks (Fig. 6, line G–H–I). The rocks dip at 15° to 45° to the N–NE in the Western Montagnais nappe and to the N in the Eastern Montagnais nappe (Fig. 3). The gabbro sills are massive or stratified; in some cases the gabbro is affected by retraction fracture systems. The basalt flows are massive or pillowed. Bacchus siltstone and sandstone form 2–5 m-thick layered packages between the gabbro sills and basalt flows.

The Montagnais nappes are affected by different sets of faults. Structural elements related to nappe emplacement are less preserved. Second-order NW–SE-striking thrust faults dipping to the NE (N352/66, striation N82/66) occur in the Montagnais gabbro in the hanging wall of the frontal Argencourt Fault. Horizontal, 3–4 cm-thick veins filled with vertically grown fibrous zeolite occur in basalt at the top of the Western Montagnais nappe (Fig. 3, area 3) and could be associated with the major shortening phase, thus indicating a horizontal orientation of the main tectonic stress. Systems of subvertical, metre-scale displaced N–S right-lateral strike-slip faults and minor W–E left-lateral strike-slip faults were observed in the mafic rocks of the nappes. The most dominant structural features in the Montagnais nappes are the N–S high-angle normal faults (Fig. 9a) and NNE–SSW extensional shear zones (Fig. 9b). The normal faults dip generally to the E in the Western Montagnais nappe and to the W in the Eastern Montagnais nappe (Fig. 3 and Fig. 6, area 3). The N–S high-angle normal faults were likely emplaced during the late extensional tectonic phase as they displace the major faults bounding the Montagnais nappes, such as the Argencourt, Bertin and Romanet faults (Fig. 3).

Wheeler Allochthonous Zone

The Wheeler allochthonous zone (Fig. 2a) includes Paleoproterozoic sedimentary rocks of the Seward, Pistolet and

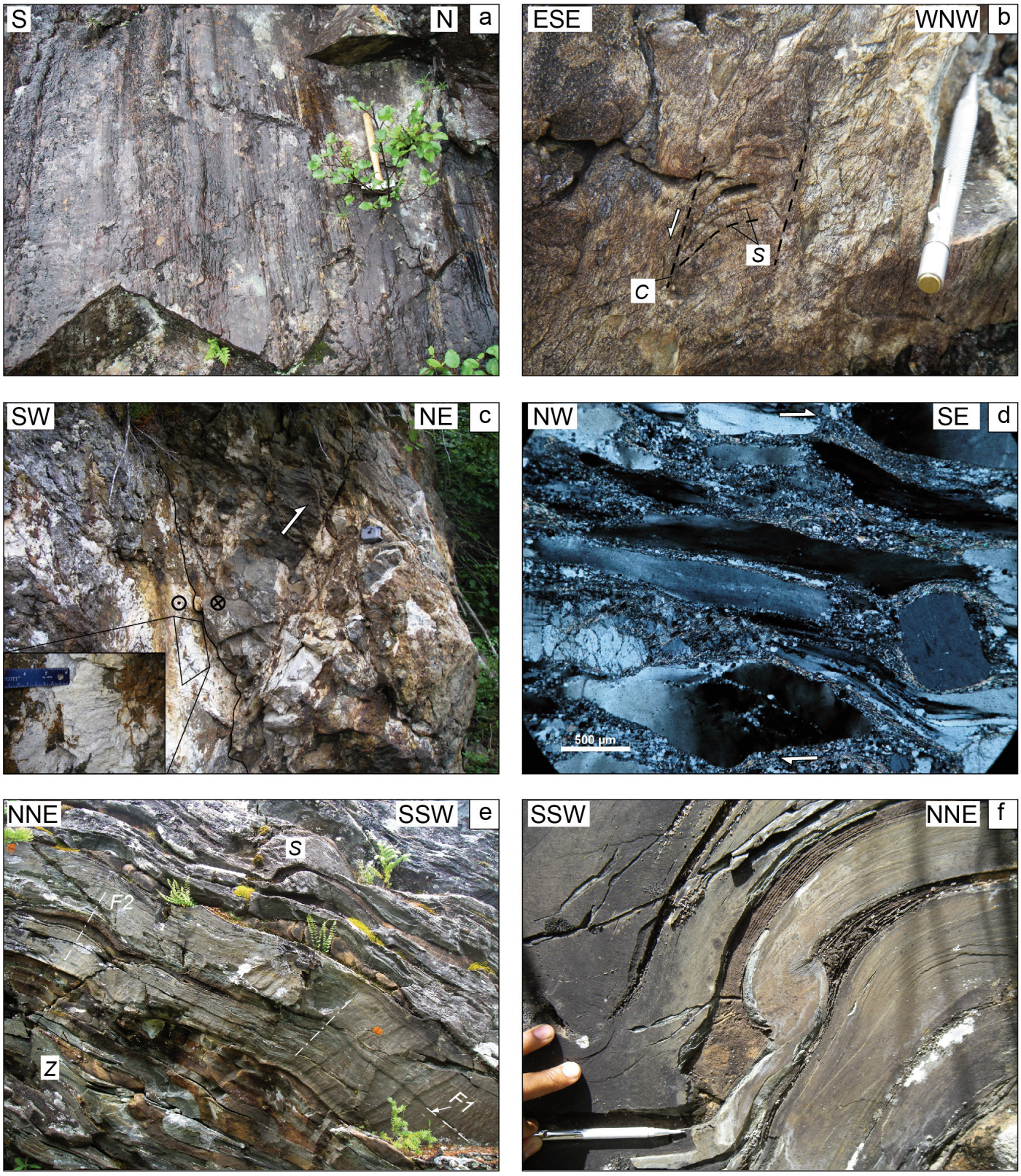

Figure 9. Structural elements of the Howse (a, b) and Wheeler (c, f) zones (areas 3−5 of Figure 3): (a) striations on the north−south-striking brittle normal fault in Bacchus basalt and (b) ductile SC normal shear zone in gabbro of the Western Montagnais nappe; (c) boudinaged fragments of Bacchus basalt in the NE-verging Bertin thrust fault zone that is cut by a subvertical left-lateral strike-slip fault with horizontal calcite striations; (d, e) Du Chambon tectonic slice: (d) strong mylonitic shearing of quartz sandstone of the Chaconipau Formation; (e) mesoscopic tight isoclinal fold F1 dipping to the SSW, slightly refolded by steeply inclined to the NNE folds F2 in dolomitic sandstone of the Dunphy Formation; note S and Z parasitic folds on the limbs of F1 fold; (f) S-type parasitic fold on the limb of F1 fold.

Swampy Bay groups and gneiss of Archean basement of the Wheeler dome (Dimroth 1978; Clark and Wares 2004). Two major faults, the Bertin Fault in the west and the Romanet Fault in the east, delineate the boundaries of the Wheeler zone (Figs. 3, 4). Previously, these faults were interpreted either as converging thrusts (Dimroth 1978) or as diverging normal faults bounding the Romanet horst (Clark and Wares 2004).

Bertin Fault

The Bertin Fault extends NW–SE along the western limit of the Romanet antiform, separating rocks of the Western Montagnais nappe to the SW from arkosic sandstone of the Chakonipau Formation and siliciclastic rocks and dolomite of the Dunphy Formation (Seward Group) that form the Du Chambon tectonic slice to the NE (Figs. 4, 6). The Bertin fault zone includes the NE-verging thrust faults (N114/45) reworked by the NW–SE left-lateral strike-slip faults (N302/86) (Fig. 6, area 4) observed both in the northern and southern segments of the fault zone. The thrust faults mark the contact between gabbro or pillow lavas and sedimentary rocks. Zones of tectonic breccia with boudins of gabbro or basaltic rocks within a carbonate matrix occur below the thrust contact (Fig. 9c). The S-dipping schistosity (N84/32) and mineral lineation plunging to the SW (N212/22) occur in the rocks of the Dunphy Formation in the footwall of the Bertin Fault (Fig. 4, area 4). The subvertical NW–SE left-lateral strike-slip faults (N302/86) are superimposed over the NW–SE thrust structures and display calcite-filled subhorizontal striations on the fault planes (Fig. 9c, inset). Subhorizontal striations and *en echelon* subvertical fracture systems indicating left-lateral displacement were observed at three different outcrops along the Bertin fault zone in area 4 (Figs. 4, 6, area 4). These observations allow us to interpret the Bertin Fault as a refolded thrust fault with initial D1 tectonic transport to the SW, which was reactivated as a top-to-the NE thrust during the D2 shortening phase and then experienced the NW–SE strike-slip left-lateral motion during D3 phase (Fig. 6, line H–I).

Romanet Antiform

The Romanet antiform (former Romanet horst) extends NW–SE for more than 35 km. Its width increases from about 3 km in the northwest to about 12–15 km in the southeast, at the border with the Archean Wheeler metamorphic dome (Fig. 3). The Romanet antiform is composed of a Paleoproterozoic sedimentary succession (Figs. 4, 6, Line H–I) of the Seward, Pistolet and Swampy Bay groups (Dimroth 1978; Clark 1986). Slate and sandstone of the Du Chambon Formation and dolomitic boulder conglomerate of the Romanet Formation (Fig. 2b) represent lateral facies of the Swampy Bay units exposed in the Schefferville and Cambrien tectonic zones to the west. The pelitic rocks of the upper part of the Du Chambon Formation contain albite–carbonate laminated and brecciated rocks of the Mistamisk Complex. The Montagnais gabbro and amphibolite form extended lenses of variable size in the sedimentary succession.

The older sedimentary units of the Seward Group (Chakonipau and Dunphy formations) are exposed in the Du Chambon and North Romanet tectonic slices (1 km to 4.5 km wide) along the southwest and northeast borders of the Romanet antiform dipping respectively to the southwest and northeast below the Western and Eastern Montagnais nappes (Figs. 4, 6, line H–I). The younger units of the Pistolet and Swampy Bay groups are exposed in the central part of the antiform that is about 7 km wide, within which rocks are deformed in a system of tight refolded synforms and antiforms extending WNW–ESE and verging to the SSW (Figs. 4, 6, line H–I).

Du Chambon Tectonic Slice

The Du Chambon tectonic slice (Fig. 4) is exposed in the footwall of the Bertin Fault for 28 km with a width varying from about 800 m in the northwest to 4.5 km in the southeast. The slice is composed of arkosic sandstone of the Chakonipau Formation and siliciclastic rocks and dolomite of the Dunphy Formation (Seward Group) emplaced over the rocks of Du Chambon and Uvé formations in the central zone of the Romanet antiform. Siltstone, dolomitic sandstone and dolomite of the Dunphy Formation in this slice are folded as tight isoclinal mesoscopic F1 folds with fold planes either horizontal or dipping to the SW (Fig. 9e). The mesoscopic folds are about 1–1.5 m wide and about 3–4 m in amplitude. The parallel limbs of the isoclinal folds can be distinguished by the presence of S- and Z-type parasitic folds (Fig. 9e) and microfolds in more ductile dolomitic beds jammed between more rigid siliciclastic sandstone (Fig. 9f). The F1 fold limbs and schistosity SC1 (Fig. 6, area 5) run parallel to the axial plane and are either subhorizontal or dip gently to moderately to the WSW (N97/37), whereas the microfold axes plunge gently to the SE (N145/28). Arkosic sandstone of the Chakonipau Formation underwent ductile shear deformation and is characterized by the presence of SC1 shear bands (Fig. 9d) and mylonitic stretching lineation plunging to the SE (N132/27) (Fig. 6, area 5). Detrital quartz grains are flattened, stretched and bent within a fine-grained quartz–mica matrix. The overturned F1 isoclinal folds are refolded by N–S upright small-amplitude (25–30 cm) F2 folds with subhorizontal axes N96/14 (Fig. 9e) and cut by NNE-verging thrust faults (N95/42) (Fig. 6, line H–I). These observations support our interpretation that the overturned SW-dipping Du Chambon tectonic slice likely represents the sheared base of the sedimentary succession deformed during the D1 deformation phase (Montagnais nappe emplacement) and subsequently refolded during the D2 shortening phase.

Core of the Romanet Antiform

The core of the Romanet antiform is made up of predominantly sedimentary rocks deformed in refolded WNW–ESE-striking antiforms and synforms that plunge to the WNW (Fig. 4). The older units of the Milamar and Lace Lake formations are exposed in the ESE of the core surrounding Archean rocks of the Wheeler metamorphic dome (Fig. 3). The younger units of the Alder-Uvé formations and Du Chambon-Romanet formations occur to the WNW and on the northeast and southwest borders of the core (Fig. 4).

The core of the Romanet antiform represents a large-scale recumbent isoclinal F1 syncline refolded by steeply (65°–76°) inclined SSW-verging F2 folds and cut by the WNW–ESE thrusts and normal faults (Fig. 6, line H–I). The core of the recumbent F1 syncline is composed of graphitic slate and dolomitic quartzite of the Du Chambon Formation containing lenses of the Montagnais gabbro and fragments of albite–carbonate rocks and breccia of the Mistamisk Complex. The upper limb of the F1 syncline is deeply eroded and the lower limb consists of rocks of the Pistolet and Seward groups. The F1 syncline is broken by WNW–ESE faults into three longitudinal segments (Fig. 4); the middle segment is uplifted and thrust over the southwestern one; the northeastern segment is downthrown along a NW–SE normal fault (Fig. 6, line H–I).

The mesoscopic F2 folds are about 600–800 m wide (Fig. 6, line H–I) and are accompanied by about 12–15 m wide secondary folds (Fig. 10a) and by 10–20 cm-scale parasitic folds (Fig. 10b). Normal and reverse bedding (N279/56) on limbs of F2 folds is recognized by stromatolite structures in dolomite, cross-bedding orientation in sandstone and schistosity–bedding relationships in shale units. The intersection lineation and F2 fold axes (Fig. 10b) are subhorizontal and gently plunge to the WNW and ESE (Fig 6, area 6). Rocks on the F2 limbs are sheared to different extents: stromatolite beds or cross-bedded sandstone beds with no grain flattening grade into highly strained rocks. Quartzite and dolomitic quartz sandstone are partially or completely recrystallized showing microstructures of recrystallized elongate quartz grains with quartz directional overgrowths in preferred orientations surrounded by ribbons of newly formed isometric fine quartz grains and/or sub-parallel mica foliae that define the microscopic fabric (Fig. 10c). The boulders (up to 1 m) of dolomitic sandstone and dolomite in conglomerate of the Romanet Formation locally remain undeformed but strongly flattened in high-strain deformation zones (Fig. 10d, e). The dolomitic quartz sandstone matrix of stretched conglomerate is recrystallized with quartz clasts surrounded by fine-grained quartz bands and mica foliae aligned between gravel-size quartz clasts parallel to the schistosity plane. The high-angle reverse schistosity SC2 in the rocks of the Romanet antiform (Fig. 6, area 6) dips to the NNE (N285/66), parallel to the axial planes of the SSW-verging F2 folds and corresponds to the D2 shortening deformation phase.

The high-angle schistosity SC2 dipping to the NNE is overprinted by a subhorizontal crenulation cleavage S3 (Fig. 10f) that occurs in the Lace Lake slate below the Romanet boulder conglomerate in the northeast of the Romanet antiform (Fig. 6, area 7b) and indicates vertical orientation of the main stress during D3 normal faulting (Fig. 6, line H–I).

The Romanet Fault Zone

The footwall of the Romanet fault zone (400–800 m wide) is exposed along the southern and northern shores of the Romanet River and is described here as the North Romanet tectonic slice (Fig. 4). It is composed of folded and sheared slate and mylonitic quartz–mica schist of the Lace Lake Formation and dolomite of the Dunphy Formation that were emplaced to the southwest over boulder conglomerate of the Romanet Formation (Fig. 6, line H–I). The mylonitic schist of the Lace Lake Formation in the North Romanet tectonic slice is characterized by the development of high-angle dextral ductile shear zones (Fig. 11a–d) and subhorizontal to low-angle mineral lineations (Fig. 11e, f). The dextral SC-C' shear zones are oriented WNW–ESE (SC N284/70, C' N298/66) and the mineral lineations and fold axes plunge to the WNW (N305/33) (Figs. 4, 6, area 7b). The extensional C' shear bands, quartz boudins and microfolds in mylonite indicate a dextral sense of shearing (Fig. 11a, c, d). Axes of cylindrical F1 microfolds gently plunge to the WNW (Fig. 11b). The low-angle mineral lineation is subparallel to the fold axes and to the orogen and indicates top-to-the-east tectonic transport during the early phase of oblique convergence. The dolomite and dolomitic quartz sandstone of the Dunphy Formation in the North Romanet tectonic slice are thrust to the SSW over the mylonitic schist of the Lace Lake Formation (Fig. 6, line H–I) and are characterized by a WNW–ESE high-angle schistosity dipping to the NNE (N290/50–52). W–E extended lenses of amphibolite and phlogopite gabbro with carbonate-altered brecciated zones occur in the North Romanet tectonic slice.

The hanging wall of the Romanet fault zone is exposed on the north shore of the Romanet River (Fig. 4, area 7a). It is characterized by a series of NW–SE high-angle normal faults and shear zones developed in the mafic rocks of the Bacchus Formation and Montagnais Group along the boundary with the sedimentary rocks of the North Romanet slice. The faults dip to the NE (N292/61) (Fig. 6, area 7a), and fault surfaces are characterized by undulations and striations (Fig. 12a) indicating normal-fault displacement. The siliciclastic rocks interbedded with pillowed basalt are affected by semi-brittle normal faulting (Fig. 12b). The steep normal SC shear bands display a low-angle schistosity (S) dipping to the N–NE (N295/64). The gabbro and basalt in the fault zones are stretched and boudinaged; within high-strain normal ductile shear zones basalt (Fig. 12c) and graphitic slate (Fig. 12d) are mylonitized with development of SC-C' extensional shear bands. The normal fault striations, mineral lineations and secondary fold axes plunge to the NNE (N18/46) indicating a SW–NE orientation of extension (Fig. 6, area 7a).

In the transition zone between the footwall and hanging wall of the Romanet fault zone, the initial reverse movement is identified by preserved reverse SC1 shear bands (N270/50) and by micro-folds in quartz–chlorite schist (Fig. 12e, f) of the Lace Lake Formation.

The observations described here allow us to interpret the Romanet Fault as a fault zone with combined kinematics (Fig. 6) of top-to-the SSW thrusting and dextral shearing in the footwall that were likely continuous during the D1–D3 deformation phases and top-to-the NE normal faulting that occurred in the hanging wall during the D3 extensional phase.

Hence, the observations of fault kinematics along the Bertin and Romanet faults and internal structure of the Wheeler allochthonous zone support the interpretation of an antiform, and the Romanet horst is therefore reinterpreted here as the Romanet antiform. This structure is interpreted as

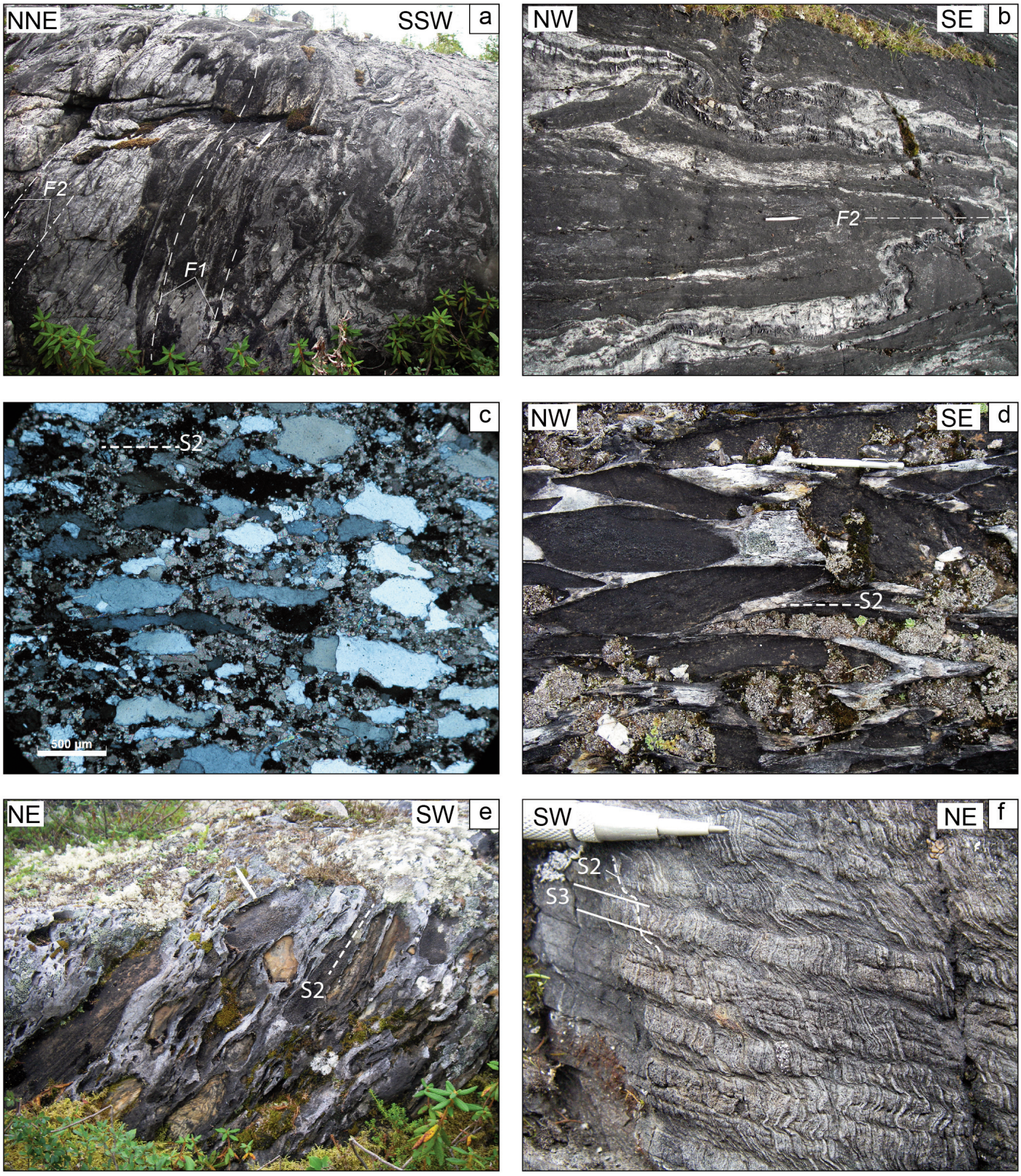

Figure 10. Structural elements of the Romanet antiform (areas 6 and 7b of Figure 4): (a–c) isoclinal folds F1 refolded by SSW-verging steeply inclined F2 folds (a); with subhorizontal axes (b); formed by dolomitic quartz sandstone of the Alder Formation, area 6; thin section of sheared matrix of Alder dolomitic sandstone (c) is characterized by elongate quartz grains with directional overgrowth in high-strain zones; (d–e) flattened boulders of dolomitic sandstone in Romanet conglomerate (d); with schistosity dipping to the NE (e); (f) subhorizontal crenulation cleavage S3 refolding steep NE-dipping schistosity S2 in slate of the Lace Lake Formation, zone 7b.

http://www.dx.doi.org/10.12789/geocanj.2019.46.143

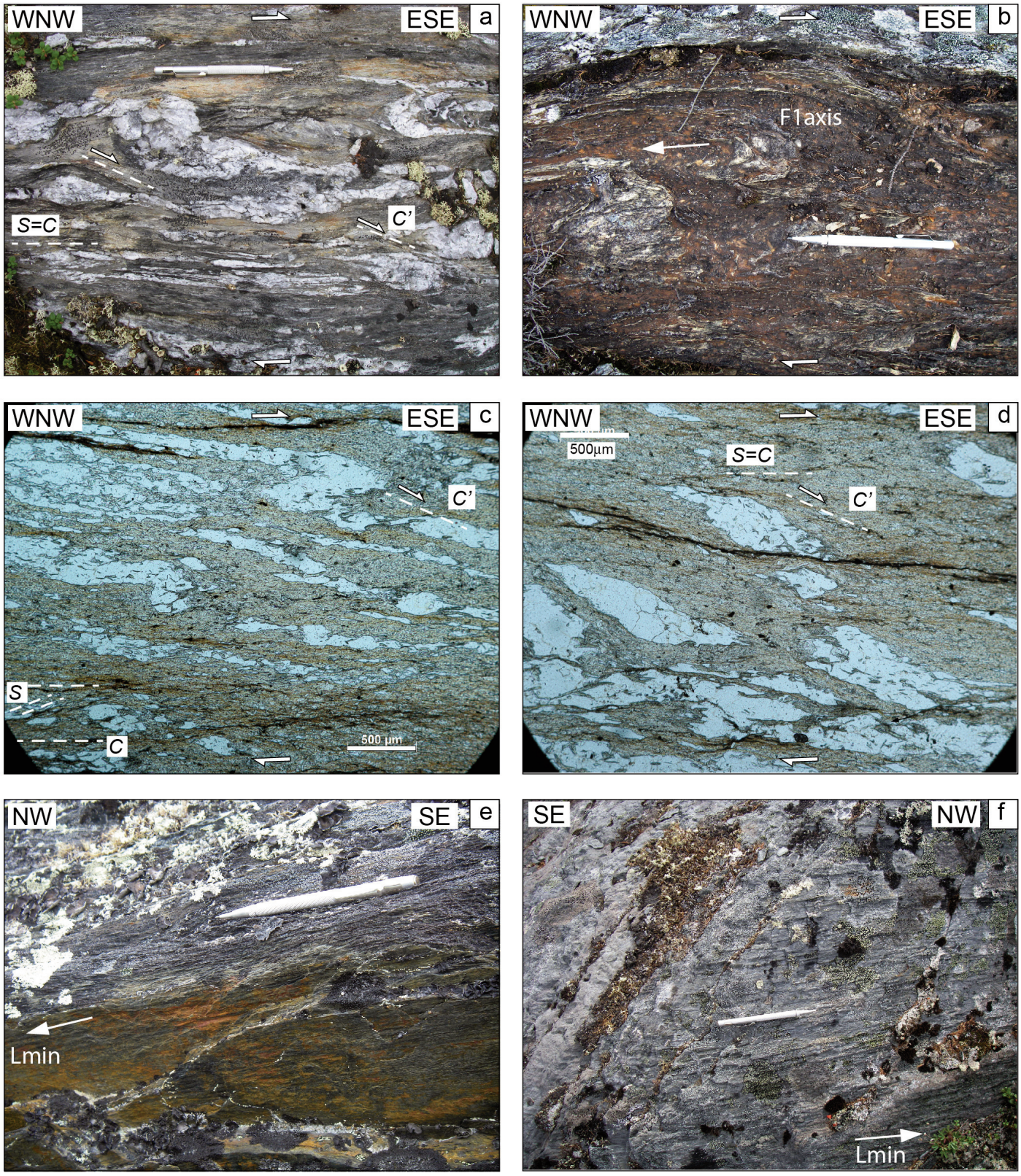

Figure 11. Structural elements of the WNW–ESE dextral mylonitic shear zone in the Lace Lake quartz–mica schist and slate in the footwall of the Romanet Fault (area 7b of Figure 4): (a) SC-C' dextral shear bands and quartz microfolds; (b) cylindrical F1 folds with axes gently plunging to the WNW; (c, d) thin section views of SC-C' dextral shear bands; (e, f) low-angle and subhorizontal stretching mineral lineations plunging to the WNW.

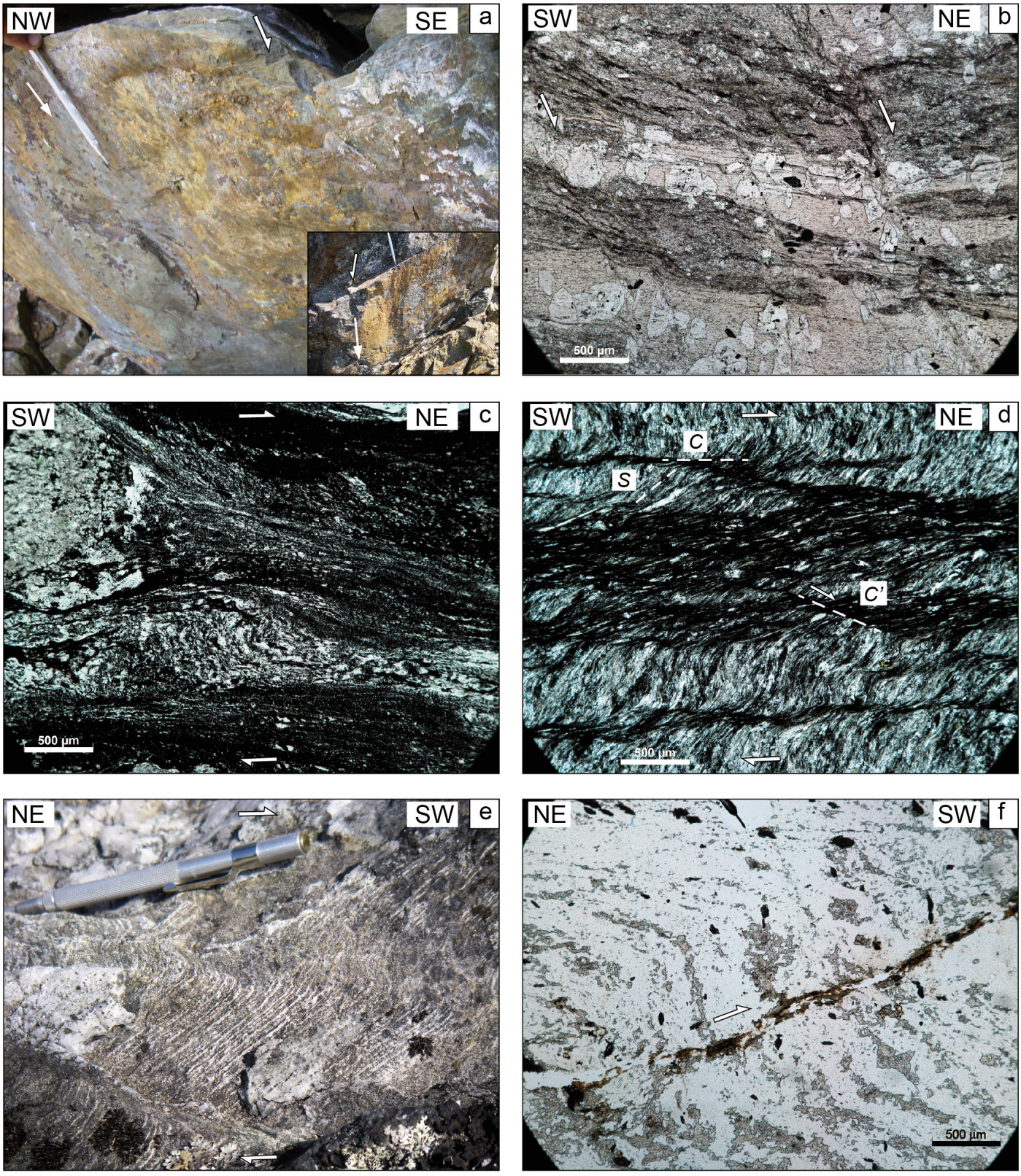

Figure 12. Structural elements of the hanging wall of the Romanet Fault (areas 7a of Figure 4): (a, b) outcrop (a) and thin-section (b) view of normal faults in the sheared Bacchus basalt and sedimentary rocks; (c, d) SC-C' normal shear bands in mylonitized Bacchus basalt (c) and graphitic slate (d); (e, f) outcrop (e) and thin section (f) view of reverse thrusting and microfolding in quartz–chlorite schist of the Lace Lake Formation in the transition zone between the footwall and hanging wall of the Romanet fault zone.

http://www.dx.doi.org/10.12789/geocanj.2019.46.143

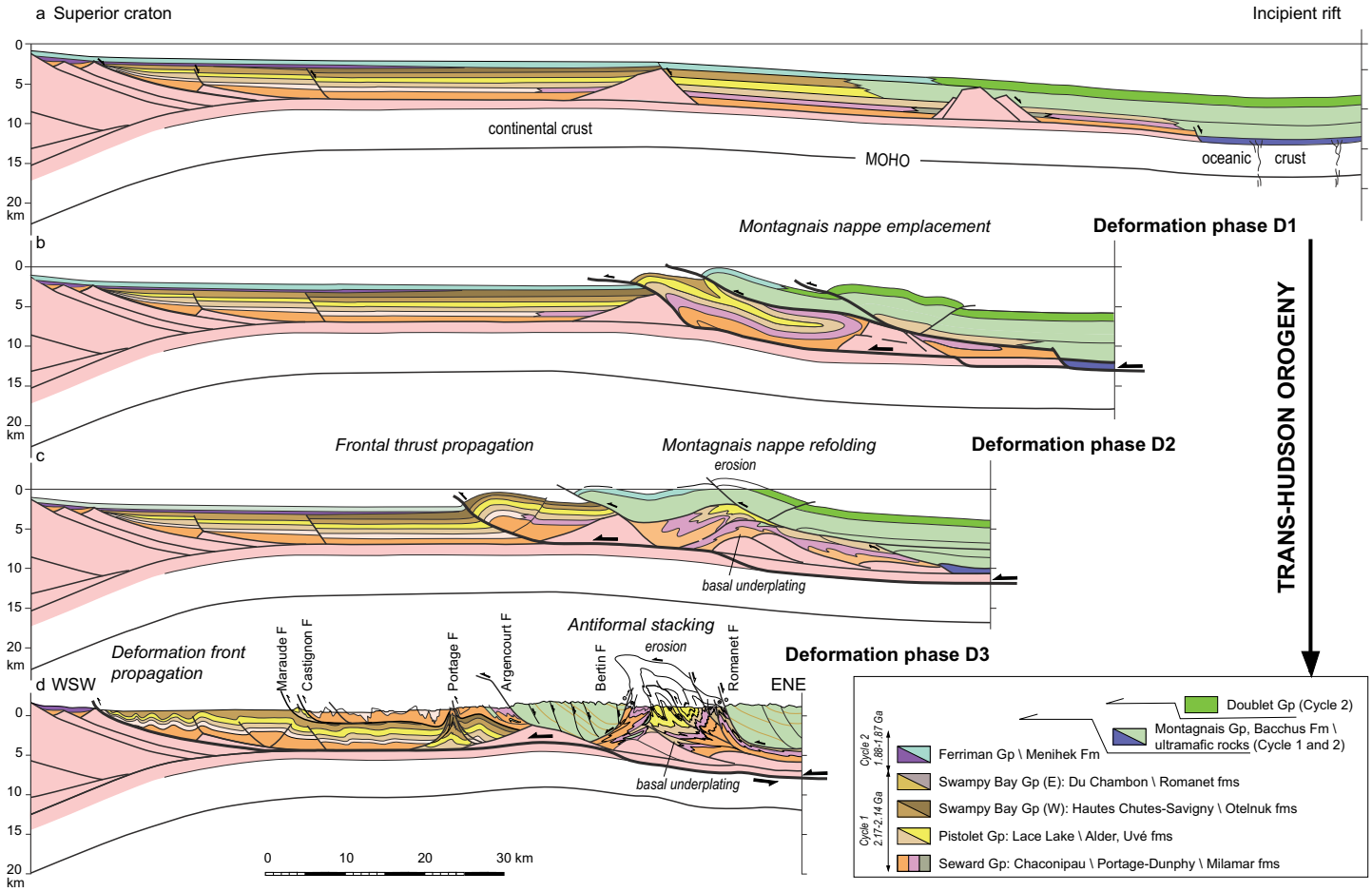

Figure 13. 2D reconstruction of initial settings and principal deformation phases D1−D3 of the Central Labrador Trough during the Trans-Hudson orogeny.

an antiformal stack formed through the combination of basal underplating, erosion and tectonic exhumation of Paleoproterozoic sedimentary rocks below the Montagnais mafic nappe in the rear part of the thrust wedge (Fig. 6). The Western and Eastern Montagnais nappes represent an initial single nappe of mafic rocks emplaced over the Paleoproterozoic sedimentary succession that during the nappe propagation was deformed into a large-scale overturned isoclinal fold with older units of the Seward Group tectonically underplating the mafic rocks in the nappe. This interpretation helps to explain the observation that highly stretched and refolded into isoclinal folds mylonitized rocks of the Chakonipau and Dunphy formations form the Du Chambon and North Romanet tectonic slices located immediately below the nappes (Figs. 4, 6). The younger sedimentary units of the Pistolet and Swampy Bay groups form a large-scale isoclinal F1 syncline in the core of the Romanet antiform that was refolded by the upright F2 folds and cut by WSW-verging thrusts under continuing shortening and basal underplating. Normal faults along the NNE boundary of the Romanet antiform (Fig. 6) likely accommodated antiformal stacking and exhumation in the core of the antiform stimulated by syntectonic erosion. The specific structures resulting from these processes at different deformation phases are described in the next section.

PRINCIPAL PHASES OF DEFORMATION

It is recognized that the principal stages of the tectonic evolution of the NQO involved: (1a) 2.2–2.1 Ga incipient crustal rifting of Superior craton; (1b) 1.88−1.87 Ga renewed rifting phase; (2) 1.82–1.77 Ga initial thrusting and collision between the Archean Superior craton and the Archean block of the Core Zone during a dextral transpression stage (Machado et al. 1989; Perreault and Hynes 1990; Skulski et al. 1993; Machado et al. 1997; Wardle et al. 2002; Clark and Wares 2004; Corrigan et al. 2018).

The tectonic setting during the phase of incipient crustal rifting can be compared to the geometry of the Galicia continental margin (Boillot and Froitzheim 2001) and was likely characterized by the presence of extended and thinned continental crust between individual thicker crustal blocks at the margin of the Superior craton and an open-marine incipient 'rift basin' (Fig. 13a). This suggestion is supported by the faulted structure described above of Archean gneiss basement of the Superior craton in the Lac Cambrien rift zone (Fig. 2a) and presence of the detached crustal blocks of Archean granite-gneiss basement (A) exposed in the lac Canichiko area of the Schefferville zone and lac Colombet area of the Howse zone (Dimroth 1978; Clark and Wares 2004). These blocks can be considered as an analog for the inferred detached basement

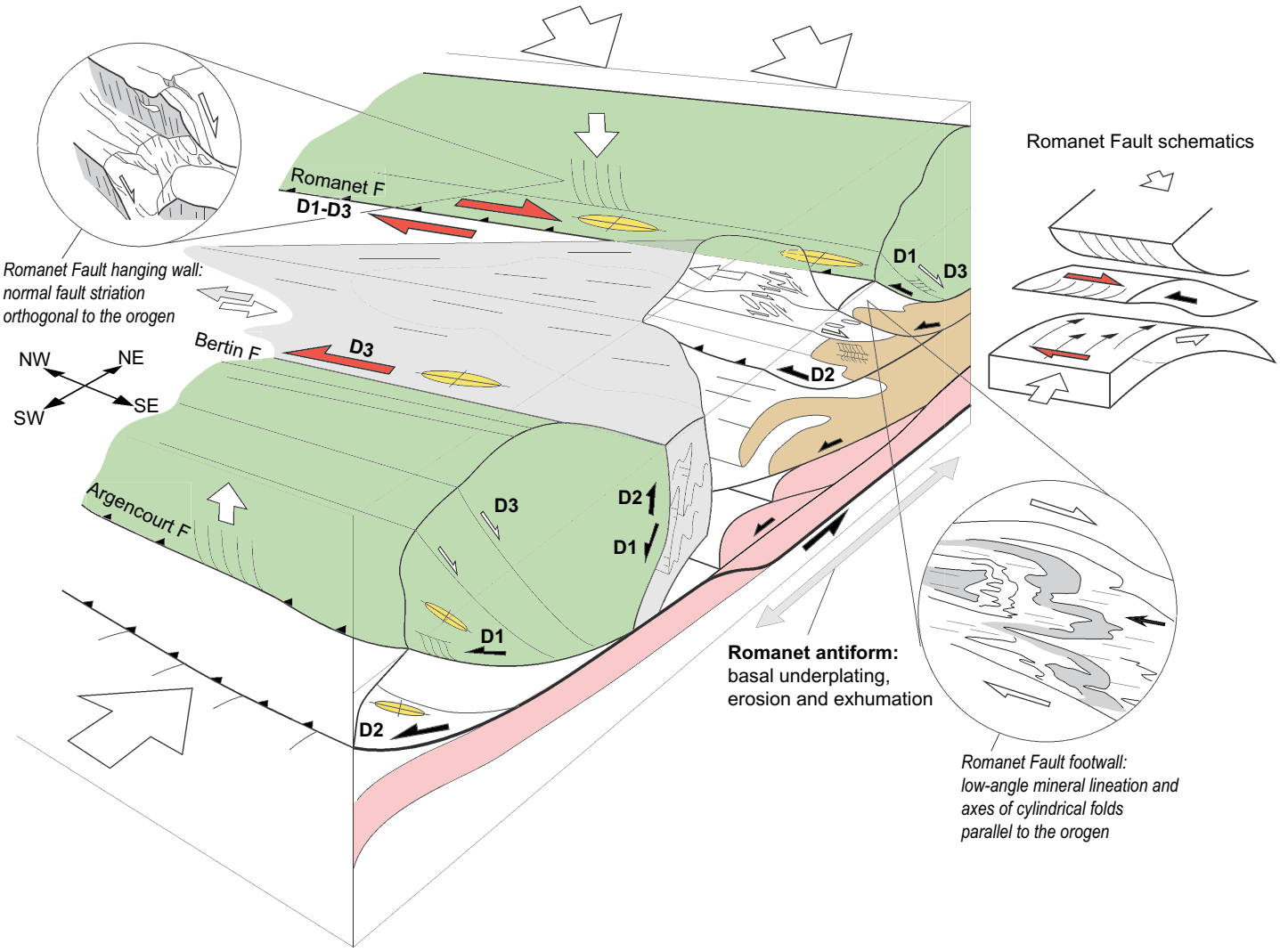

Figure 14. 3D model of tectonic structure of the Wheeler zone showing principal structural elements of the Montagnais nappes and Romanet antiform. The longitudinal progressive increase in the amount of exhumation from the NW to the SE in the antiform is likely related to along-strike variation of shortening and erosion increasing to the southeast.

block below the frontal slices of the Howse zone (Fig. 6). The crustal blocks underplated below the Romanet antiform (Fig. 6) are inferred from the nearby location of the Wheeler dome (Fig. 2a), which is considered to be bounded at the base by a major W-verging decollement (Clark and Wares 2004).

Our structural observations in the Central Labrador Trough support several episodes of thrusting and strike-slip deformation that occurred during the collisional stage followed by extensional shearing and normal faulting during the late phases of syncollisional shortening (Fig. 13b–d).

D1 Nappe Emplacement

The D1 phase is characterized by westward (in present-day coordinates) emplacement of the Montagnais mafic nappe over the Paleoproterozoic sedimentary succession with subsequent decollements along shaly and/or dolomitic units and the formation of a large-scale recumbent isoclinal F1 fold (Fig. 13b). Thrust emplacement under dextral transpressional conditions resulted in the development of right-lateral mylonitic shearing and the top-to-the WNW subhorizontal stretching mineral lineation parallel to the orogen in the footwall of the Romanet Fault (Fig. 6, area 7b), and reverse shearing in the transition zone between the footwall and hanging wall of the Romanet Fault (Fig. 14). These deformation events are recorded in the Lace Lake quartz–mica schist (Figs. 11a–d, 12e, f) of the North Romanet slice in the rear part of the thrust wedge. Mylonitic shearing (Figs. 9d, 10c) and formation of recumbent southwest-dipping isoclinal F1 folds (Fig. 9e) occurred during this stage in the Chaconipau sandstone and Dunphy dolomite of the Wheeler zone (Fig. 14). D1-related relics of the gabbro nappes (Fig. 5, lines A–B, C–D) and associated brecciation and schistosity of the Lace Lake shale in the nappe footwall (Fig. 7d) are recognized in the Minowean syncline (Schefferville zone).

D2 Nappe Refolding and Forward Thrust Propagation

During the D2 phase, the deformation front propagated southwestward with emplacement of SW-verging steep thrusts and moderately inclined folds in the Paleoproterozoic succession (Fig. 13c) in the frontal part of the thrust wedge (Schefferville zone). Top-to-SW reverse SC2 shear bands in the Argencourt Fault (Fig. 8e) and striations at thrust surfaces, steep schistosity SC2 dipping to the NE (Fig. 8f), NW–SE intersection lineation and subhorizontal fold axes (Fig. 5, areas 1, 2) are consistent with a SW (N220°) direction of tectonic transport. Deformation propagation continued during the D3 phase resulting in emplacement of the Portage and Castignon slices along the detachment in shale of the Swampy Bay Group in the Schefferville parautochthonous zone (Fig. 13d). Eventually, minor folding and local thrust faulting affected the autochthonous Cambrien zone. The development of the Swampy Bay dextral mylonitic shear zone (Fig. 8a, b) and dextral transpressional displacement along the Portage Fault (Fig. 3) characterizing the D2–D3 phase may reflect strain partitioning during oblique convergence between the Superior craton and the Core Zone during the Trans-Hudson orogeny.

Continuous underplating at the rear part of the thrust wedge (Wheeler zone) resulted in upward bending of the Montagnais nappe (Fig. 13c), refolding of recumbent isoclinal F1 folds as upright and SSW-verging inclined F2 folds with subhorizontal axes (Fig. 10a, b), and development of a steep schistosity (Fig. 10e) and thrusts dipping to the NNE (Fig. 6, area 6). The Bertin Fault and the shear detachment at the base of the Du Chambon slice were bent, plunging to the SW (Fig. 6, line H–I) and under continuing shortening they were reactivated as NE-verging reverse faults (Fig. 6, areas 4 and 5).

D3 Underplating, Antiformal Stacking, Erosion, Extensional Shearing and Normal Faulting

During the D3 phase, underplating and growth of the antiformal stack combined with localized erosion in the rear part of the thrust wedge resulted in exhumation of sedimentary rocks of the Romanet antiform (Fig. 13d). The amount of erosion and exhumation likely varied along the strike of the orogen in the Romanet area with maximum erosion and uplift occurring in the SE and decreasing to the WNW, where higher structural levels are preserved (Fig. 14). The deeper levels composed of older metasedimentary units of the Lace Lake and Milamar formations are exhumed in the southeast, close to the Archean gneiss basement of the Wheeler dome (Fig. 3). To the NW, lesser amounts of exhumation and erosion resulted in preservation of younger sedimentary units of the Pistolet and Swampy Bay groups. Higher amounts of exhumation in the southeast of the Romanet antiform resulted in superimposed left-lateral strike-slip faulting along the Bertin fault zone (Fig. 9c) and in continued right-lateral displacement in the footwall of the Romanet Fault (Fig. 11a–d).

The continued syncollisional underplating and exhumation in the Romanet antiform resulted in the development of extensional structures along the northeastern antiform boundary (Fig. 13d). A NE-dipping normal fault bounds the downthrown block composed of the Romanet conglomerate (Fig. 6) at the northeastern limit of the central zone. A subhorizontal S3 crenulation cleavage refolds the steep NNE-dipping S2 schistosity (Fig. 10f) in the Lace Lake slate, northeast of the Romanet antiform. Extensional shear zones and brittle normal faults with northeast-plunging mineral lineations and striations (Fig. 6, area 7a) occur in the hanging wall of the Romanet Fault (Fig. 12a–d).

Late N–S normal faults and shear zones cut mafic rocks of the Montagnais nappes (Fig. 9a, b) and the sedimentary rocks below the nappes in the frontal part of the thrust wedge (Figs. 3, 6, line G–H–I). The NW–SE brittle and semi-brittle normal faults occur in shale of the Lace Lake Formation below the frontal gabbro slice nappe (Fig. 8c, d) and in quartz sandstone of the Alder Formation (Fig. 7f) on the overturned limb of the Minowean syncline (Fig. 5, line A–B). This late normal faulting could result from collapse following the emplacement of the thick gabbro nappe over the parautochthonous sedimentary rocks.

DISCUSSION

Nappe Emplacement and Thrusting

The main phases of deformation related to the Trans-Hudson orogeny in the Central Labrador Trough (Fig. 13b–d) described above can be correlated with synchronous phases in the northern Labrador Trough. The major deformation events related to shortening in the northern Labrador Trough involved: D1 basal decollement, D2 northwest transport of basement-cored Pennine-style nappes, and D3 main stage of compression. The westward transport along D1 decollement planes is estimated to range from 25 to 50 km (Goulet 1995). The SW and WSW direction of transport was probably continuous in the foreland during D2 and D3 and should not be considered as discrete events (Moorhead and Hynes 1990; Wares and Goutier 1990; Goulet 1995). An early episode of low-angle in-sequence thrusting and a later phase of major high-angle out-of-sequence thrusting have been distinguished in the structural evolution of the western foreland both in the northern (Wares and Goutier 1990) and in the central (this study) segments of NQO. In the north, northwest-trending *en echelon* allochthonous domes of Archean (2883–2868 Ma, zircon) basement gneiss (Machado et al. 1989) are exposed in cores of the Boulder and Moyer antiforms and Renia synform (Fig. 1) between the two steep east-dipping Lac Rachel and Lac Olmstead dextral strike-slip faults (Moorhead and Hynes 1990). These structures represent large west-verging, basement-cored nappes developed through the decollement at the basement-cover interface and were refolded during later northwest- and southwest-directed thrust fold phases (Moorhead and Hynes 1990). Similarly, in the Central Labrador Trough, basal underplating and antiformal stacking of sedimentary cover and inferred detached crustal blocks (Fig. 13d) occurred below the Montagnais nappe in the rear part of the thrust wedge and resulted in nappe refolding and out-of-sequence high-angle thrusting during the D2–D3 continuous phases of progressive shortening (Fig. 13c, d). An analog basal detachment is inferred by Clark and Wares (2004) at the base of the

Wheeler dome of Archean basement gneiss (2668 Ma, zircon) (Rayner et al. 2017; Charette et al. 2017).

According to numerical and analog modelling results, the occurrence of frontal and basal accretion in a thrust wedge is influenced by the rheology of the material, surface processes and the balance of material flux (Davis et al. 1983; Selzer at al. 2008; Malavieille 2010; Pfiffner 2017). In sandbox models with a decollement layer, the processes of basal underplating, nappe stacking, syncollisional exhumation and extension above the uplifted core zone are favoured by syntectonic surface erosion (Konstantinovskaia and Malavieille 2005; Bonnet et al. 2007; Konstantinovskaya and Malavieille 2011).

Strike-slip Faulting

A series of NW−SE dextral strike-slip faults, namely the Lac Rachel, Lac Olmstead, Lac Turcotte, and Lac Tudor faults (Fig. 1) is recognized on the eastern border of the NQO (Girard 1990; Moorhead and Hynes 1990; Goulet 1995; Wardle et al. 2002; Simard et al. 2013). In the hinterland of the northern segment of the orogen, the Lac Rachel and Lac Olmstead dextral strike slip faults are interpreted to be related to the D3 deformation phase, during which the D1−D2 structures were refolded to form a series of *en echelon* anticlinoria and synclinoria (Goulet 1995). The Lac Turcotte Fault represents a dextral mylonitic shear zone formed during an early deformation phase of juxtaposition of the Core Zone and Rachel-Laporte zone (Poirier et al. 1990; Perreault and Hynes 1990). The Lac Turcotte Fault probably represents a continuation of the Lac Tudor Fault in the south (Wardle et al. 2002). The Turcotte-Tudor dextral shear zone corresponds to a prominent suture related to the collision between the Superior Craton and the Core Zone (Clark and Wares 2004; Corrigan et al. 2009). The mineral lineation plunging at low angles to the southeast characterizes metamorphic rocks of both the Rachel-Laporte zone and the Core Zone that may reflect the effect of the oblique component during the D3 deformation phase of the collision (Simard et al. 2013). The displacement along the dextral strike-slip fault zones occurred between 1793 and 1783 Ma (Machado et al. 1989; Clark and Wares 2004) as a result of dextral transpression kinematics during the Trans-Hudson orogeny.

The strike-slip faults and shear zones in the Central Labrador Trough described in this study developed during different deformation phases from the hinterland to the frontal parts of the orogen. The dextral shear mylonitic zones and low-angle stretching mineral lineation parallel to the orogen that occur in the footwall of the Romanet fault zone likely record the early stages (D1) of oblique convergence between the Superior craton and the Archean crustal block of the Core Zone (Fig. 14, inset). The basal underplating and nappe refolding through D2−D3 phases resulted in antiformal stacking in the Romanet antiform, continued dextral shearing in the footwall of the Romanet fault zone and top-to-the NE thrusting along the Bertin Fault subsequently reworked as a left-lateral strike-slip fault. The left-lateral strike-slip faulting along the Bertin Fault and continued right-lateral shearing along the Romanet Fault developed as a result of longitudinally heterogeneous exhumation in the Romanet antiform (Fig. 14) during the D2−D3 phase. The Swampy Bay dextral shear zone and right-lateral displacement along the Portage Fault (Figs. 3, 5) of the Schefferville and Howse zones could also be the result of strain partitioning during the late phases (D2−D3) of shortening in the frontal part of the thrust wedge. Thus, the effect of dextral transpression during the oblique Trans-Hudson orogeny was not limited by the hinterland (Rachel-Laporte zone) but was also pronounced in the Labrador Trough (Wheeler, Howse and Schefferville zones).

Along-strike Variation of Exhumation and Shortening

Field observations and structural analysis of the Romanet antiform has shown that deeper structural levels are exhumed in the southeast, near the Wheeler dome, while shallower levels are preserved in the northwest (Fig. 14). This allows us to suggest an along-strike variation of exhumation rate in the rear part of the thrust wedge that can be explained by higher erosion and shortening rates in the southeastern segment of the thrust wedge as compared to the northwestern segment. In other words, higher shortening in the southeastern segment resulted in higher amounts of basal underplating that involved detached crustal blocks of Archean basement below the core of the Romanet antiform (Fig. 13d) and contributed to higher rates of erosion and exhumation in the southeastern segment (Fig. 14). If this interpretation is valid, the Wheeler dome, located at the extreme southeast point of the Romanet antiform (Figs. 2a, 3), may represent a detached and underplated crustal block of Archean basement that, together with its sedimentary cover (Milamar meta-conglomerate), experienced the highest amounts of differential exhumation in the Wheeler zone during the Trans-Hudsonian orogeny. The proposed model requires a validation by further regional structural and geochronological studies. An analog structural model was proposed by Rosenberg et al. (2015) for the Alps. Those authors have shown that along-strike gradients of collisional shortening in the Central and Eastern Alps may result in longitudinal variation of the erosion and exhumation rates. Stronger shortening coincides with a thicker eroded rock column and higher rate of exhumation. This model can be applied to explain the structural features of the Central Labrador Trough.

Late Normal Faulting

Extension in collisional orogens may be related either to late orogenic extension and collapse or to local crustal shortening (Malavieille 1993). The late orogenic extension model involves the development of normal shear zones and the growth of a metamorphic core complex (Van Den Dreissche and Brun 1989; Echtler and Malavieille 1990). Other models consider the occurrence of detachments in collisional orogens during the unroofing and thinning of thickened crust during shortening (Malavieille 1993; Matte 2007).

In the Central Labrador Trough, the D3 extensional phase is recognized for the first time and is related to different processes. Along the Romanet fault zone, normal faults and shear zones occur in the hanging wall with stretching lineations and striations plunging to the northeast, orthogonal to the orogen, in contrast to the stretching mineral lineation in the

footwall, which gently plunges to the WNW, subparallel to the orogen (Fig. 14). Such structures are typical of orogens with oblique tectonics such as the Western Alps, Taiwan and the Canadian Rockies and are formed during two distinct phases (Ellis and Watkinson 1987): an early footwall deformation with stretching lineation parallel to the orogen reflecting high oblique strain of oblique subduction, and a later hanging wall deformation with structures orthogonal to the orogen reflecting imbrication and exhumation processes.

In the northeastern part of the Romanet antiform, the northeast-dipping normal faults and subhorizontal S3 crenulation cleavage (Figs. 10f, 14) likely reflect a syn-convergent mechanism of extension that combines simultaneous uplift and exhumation induced by local basal underplating of detached units and erosion during convergence. Based on analog experiments (Konstantinovskaia and Malavieille 2005; Malavieille 2010; Malavieille and Konstantinovskaya 2010; Konstantinovskaya and Malavieille 2011), it is possible to suggest that normal faulting could be the result of the kinematic effect of vertical shears induced by strain partitioning in the orogenic wedge. Such partitioning is the direct consequence of upper crustal underplating processes combined with surface erosion and induces strong uplift in discrete areas. Differential motion of underplated crustal units relative to surrounding material induces vertical shearing and as a consequence strong stretching and layer-parallel thinning of the stacked tectonic units. At depth these zones are characterized by the development of normal shear zones that evolved to brittle normal faults when reaching upper crustal domains during continuous syn-convergent erosion assisted by uplift (Malavieille and Konstantinovskaya 2010).

The late brittle normal faulting in the Montagnais nappes and in the sedimentary units below the frontal nappes (Figs. 3, 5) in the frontal (western) part of the thrust wedge (Minowean area) is likely related to stress relaxation after the emplacement of voluminous gabbro nappes over the Proterozoic sedimentary succession.

Further detailed structural, mineralogical and geochronological studies in the Central Labrador Trough would help to quantify timing of the deformation phases, including the antiformal stacking and exhumation phase and the newly defined D3 extensional phase, and to characterize structural control on fluid circulation and mineralization processes relevant for mineral prospecting in the area. In particular, structural and geochronological studies of lenses of amphibolite and phlogopite gabbro in the footwall of the Romanet Fault and greenschist of the Milamar Formation along the southwestern border of the Wheeler dome could contribute to our understanding of the mylonitic deformation during the early D1 deformation phase of nappe emplacement and decollement propagation at the base of the detached Archean basement block.

CONCLUSIONS

Field structural observations carried out along the ca. 70 km long W−E Minowean-Romanet transect in the Central Labrador Trough have helped to recognize three distinct deformation phases during the Trans-Hudson orogeny that include not only southwestward thrusting (D1−D3) but also the newly established strike-slip (D1−D3) and extensional (D3) tectonics that developed under various settings in the frontal (western) and rear (eastern) parts of the orogen.

In the east, the low-angle mineral lineation, the axes of cylindrical folds and the dextral mylonitic shear zones in the footwall of the Romanet Fault are oriented subparallel to the orogen and reflect the early D1 phase of oblique convergence. The mineral lineations and striations of normal faults and shear zones in the hanging wall of the Romanet Fault are oriented orthogonally to the orogen and correspond to the later phase (D3) of exhumation driven by the combined effects of erosion and underplating. The increasing degree of exhumation along the Romanet antiform from northwest to southeast is explained by a model of strain partitioning and differential exhumation resulting from longitudinal variations of shortening and associated higher amount of erosion in the southeast in an oblique convergence setting.

The D3 northeast-dipping normal fault and subhorizontal crenulation cleavage to the northeast of the Romanet antiform likely reflect the syn-convergent mechanism of extension that combined simultaneous uplift, vertical shearing and exhumation induced by local basal underplating and erosion during convergence. The late D3 brittle normal faults, semi-brittle and ductile shear zones in the Montagnais nappes and in the sedimentary units below the frontal nappes of the thrust wedge (Minowean area) are likely related to stress relaxation after emplacement of the voluminous gabbro nappes over the Proterozoic sedimentary succession.

ACKNOWLEDGEMENTS

The authors express their deep gratitude and remembrance to J.L. Feybesse for his contribution to the field work in the region. We thank Jacques Malavieille for internal review of the draft manuscript; Brendan Murphy, Section Editor, Andrew Hynes Tectonic Series, Andrew Kerr, Scientific Editor, and two anonymous reviewers for positive and constructive reviews, comments and suggestions that helped us to improve and considerably enhance the quality of the initial version of manuscript; Rob Raeside and Cindy Murphy for helpful edits and suggestions of the copyedited manuscript.

REFERENCES

Boillot, G., and Froitzheim, N., 2001, Non-volcanic rifted margins, continental break-up and the onset of sea-floor spreading: some outstanding questions, *in* Wilson, R.C.L., Whitmarsh, R.B., Taylor, B., and Froitzheim, N., *eds.*, Non-Volcanic Rifting of Continental Margins: A Comparison of Evidence from Land and Sea: Geological Society, London, Special Publications, v. 187, p. 9–30, https://doi.org/10.1144/GSL.SP.2001.187.01.02.

Bonnet, C., Malavieille, J., and Mosar, J., 2007, Interactions between tectonics, erosion, and sedimentation during the recent evolution of the Alpine orogen: Analogue modeling insights: Tectonics, v. 26, TC6016, https://doi.org/10.1029/2006TC002048.

Brouillette, P., 1989, Géologie de métallogénie de la région des lacs Minowean et du Portage (Fosse du Labrador): Ministère de l'Énergie et des Ressources naturelles, Québec, ET 88–06, 74 p.

Burg, J.-P., Bale, P., Brun, J.-P., and Girardeau, J., 1987, Stretching lineation and transport direction in the Ibero-Armorican arc during the Siluro–Devonian collision: Geodinamica Acta, v. 1, p. 71–87, https://doi.org/10.1080/09853111.1987.11105126.

Charette, B., Lafrance, I., and Mathieu, G., 2017, Géologie de la région du Lac Jeannin (SNRC 24Bb): Ministère de l'Énergie et des Ressources naturelles, Québec, Rapport géologique. Available from: http://gq.mines.gouv.qc.ca/rapports-geologiques/province-de-churchill/geologie-du-lac-jeannin/.

Chevé, S.R., 1985, Les indices minéralisés du lac Romanet, Fosse du Labrador :

Ministère de l'Énergie et des Ressources naturelles, Québec, ET 83–13, 60 p. Available from: http://sigeom.mines.gouv.qc.ca/.

Chevé, S.R., 1993, Cadre géologique du complexe carbonatitique du lac Castignon, Fosse du Labrador: Ministère de l'Énergie et des Ressources naturelles, Québec, MB 93–64, 100 p.

Chevé, S.R., and Machado, N., 1988, Reinvestigation of the Castignon Lake carbonatite complex, Labrador Trough, New Quebec (Abstract): Geological Association of Canada-−Mineralogical Association of Canada, Joint Annual Meeting, 1988, St. John's, Newfoundland, Abstracts, v. 13, p. 20.

Clark, T., 1984, Géologie de la région du lac Cambrien, Territoire du Nouveau Québec: Ministère de 1'Energie et des Ressources naturelles, Québec, ET 83-02, 71 p.

Clark, T., 1986, Géologie et minéralisations de la région du lac Mistamisk et de la rivière Romanet: Ministère de l'Énergie et des Ressources naturelles, Québec, PRO 87–18, 7 p.

Clarke, T., and Wares, R., 2004, Synthèse lithotectonique et métallogénique de l'orogène du Nouveau-Québec (Fosse du Labrador): Ministère de l'Énergie et des Ressources naturelles, Québec, Rapport MM 2004–01, 182 p.

Corrigan, D., Pehrsson, S., Wodicka, N., and de Kemp, E., 2009, The Paleoproterozoic Trans-Hudson Orogen: a prototype of modern accretionary processes, *in* Murphy, J.B., Keppie, J.D., and Hynes, A.J., *eds.,* Ancient Orogens and Modern Analogues: Geological Society, London, Special Publications, v. 327, p. 457−479, https://doi.org/10.1144/SP327.19.

Corrigan, D., Wodicka, N., McFarlane, C., Lafrance, I., van Rooyen, D., Bandyayera, D., and Bilodeau, C., 2018, Lithotectonic framework of the Core Zone, southeastern Churchill Province, Canada: Geoscience Canada, v. 45, p. 1−24, https://doi.org/10.12789/geocanj.2018.45.128.

Davis, D.M., Suppe, J., and Dehlen, F.A., 1983, Mechanics of fold-and-thrust belts and accretionary wedges: Journal of Geophysical Research, v. 88, p. 1153–1172, https://doi.org/10.1029/JB088iB02p01153.

Dimroth, E., 1978, Région de la Fosse du Labrador (54˚30'–56˚30'): Ministère de l'Énergie et des Ressources naturelles, Québec, RG–193, 396 p.

Dimroth, E., and Dressler, B.O., 1978, Metamorphism of the Labrador Trough, *in* Fraser, J.A., and Heywood, W.W., *eds.*, Metamorphism in the Canadian Shield: Geological Survey of Canada, Paper 78–10, p. 215–236, https://doi.org/10.4095/104534.

Dressler, B., 1979, Région de la Fosse du Labrador: Ministère de l'Énergie et des Ressources naturelles, Québec, RG–195, 136 p.

Echtler, H., and Malavieille, J., 1990, Extensional tectonics, basement uplift and Stephano-Permian collapse basin in a late Late Variscan metamorphic core complex (Montagne Noire, Southern Massif Central): Tectonophysics, v. 177, p. 125–138, https://doi.org/10.1016/0040-1951(90)90277-F.

Ellis, M., and Watkinson, A.J., 1987, Orogen-parallel extension and oblique tectonics: The relation between stretching lineations and relative plate motions: Geology, v. 15, p. 1022–1026, https://doi.org/10.1130/0091-7613(1987)15<1022:OEAOTT>2.0.CO;2.

Ellis, M.A., 1986, Structural morphology and associated strain in the central Cordillera (British Columbia and Washington): Evidence of oblique tectonics: Geology, v. 14, p. 647–650, https://doi.org/10.1130/0091-7613(1986)14<647:SMAASI>2.0.CO;2.

Findlay, J.M., Parrish, R.R., Birkett T.C., and Watanabe, D.H., 1995, U–Pb ages from the Nimish Formation and Montagnais glomeroporphyritic gabbro of the central New Québec Orogen, Canada: Canadian Journal of Earth Sciences, v. 32, p. 1208–1220, https://doi.org/10.1139/e95-099.

Girard, R., 1990, Les cisaillements latéraux dans l'arrière-pays des orogènes du Nouveau-Québec et de Torngat: Une revue: Geoscience Canada, v. 17, p. 301–304.

Goulet, N., 1995, Étude structurale, stratigraphique et géochronologique de la partie nord de la Fosse du Labrador: Ministère de l'Énergie et des Ressources naturelles, Québec, MB 95–36, 41 p. Available from: http://sigeom.mines.gouv.qc.ca/.

Goulet, N., Gapiéry, C., Mareschal, J.-C., and Machado, N., 1987, Structure, geochronology, gravity and the tectonic evolution of the northern Labrador Trough: Geological Association of Canada−Mineralogical Association of Canada, Joint Annual Meeting, Saskatoon, Saskatchewan, 1987, Program with Abstracts, v. 12, p. 48.

Hoffman, P.F., 1988, United plates of America, the birth of a craton: Early Proterozoic assembly and growth of Laurentia: Annual Review of Earth and Planetary Sciences, v. 16, p. 543–603, https://doi.org/10.1146/annurev.ea.16.050188.002551.

Hoffman, P.F., 1990, Dynamics of the tectonic assembly of the northeast Laurentia in geon 18 (1.9−1.8 Ga): Geoscience Canada, v. 17, p. 222–226.

James, D.T., and Dunning, G.R., 2000, U–Pb geochronological constraints for Paleoproterozoic evolution of the Core Zone: southeastern Churchill Province, northeastern Laurentia: Precambrian Research, v. 103, p. 31–54, https://doi.org/10.1016/S0301-9268(00)00074-7.

Karhu, J.A., and Holland, H.D., 1996, Carbon isotopes and the rise of atmospheric oxygen: Geology, v. 24, p. 867-−870, https://doi.org/10.1130/0091-7613(1996)024<0867:CIATRO>2.3.CO;2.

Konstantinovskaia, E., and Malavieille, J., 2005, Erosion and exhumation in accretionary orogens: Experimental and geological approaches: Geochemistry, Geophysics, Geosystems, v. 6, Q02006, https://doi.org/10.1029/2004GC000794.

Konstantinovskaya, E., and Malavieille, J., 2011, Thrust wedges with décollement levels and syntectonic erosion: A view from analog models: Tectonophysics, v. 502, p. 336–350, https://doi.org/10.1016/j.tecto.2011.01.020.

Lacassin, R., 1987, Kinematics of ductile shearing from outcrop to crustal scale in the Monte Rosa Nappe, Western Alps: Tectonics, v. 6, p. 69–88, https://doi.org/10.1029/TC006i001p00069.

Le Gallais, C.J., and Lavoie, S., 1982, Basin evolution of the Lower Proterozoic Kaniapiskau Supergroup, central Labrador miogeocline (Trough), Quebec: Bulletin of Canadian Petroleum Geology, v. 30, p. 150−166.

Machado, N., 1990, Timing of collisional events in the Trans-Hudson Orogen: evidence from U−Pb geochronology for the New Quebec Orogen, the Thompson Belt and the Reindeer Zone (Manitoba and Saskatchewan), *in* Lewry, J.F., and Stauffer, M.R., *eds*., The Early Proterozoic Trans-Hudson Orogen of North America: Lithotectonic Correlations and Evolution: Geological Association of Canada, Special Paper 37, p. 433−441.

Machado, N., Goulet, N., and Gariépy, C., 1989, U–Pb geochronology of reactivated Archean basement and of Hudsonian metamorphism in the northern Labrador Trough: Canadian Journal of Earth Sciences, v. 26, p. 1–15, https://doi.org/10.1139/e89-001.

Machado, N., Clark, T., David, J., and Goulet, N., 1997, U–Pb ages for magmatism and deformation in the New Quebec Orogen: Canadian Journal of Earth Sciences, v. 34, p. 716−723, https://doi.org/10.1139/e17-058.

Malavieille, J., 1993, Late orogenic extension in mountain belts: insights from the Basin and Range and the Late Paleozoic Variscan Belt: Tectonics, v. 12, p. 1115–1130, https://doi.org/10.1029/93TC01129.

Malavieille, J., 2010, Impact of erosion, sedimentation, and structural heritage on the structure and kinematics of orogenic wedges: Analog models and case studies: GSA Today, v. 20, p. 4–10, https://doi.org/10.1130/GSATG48A.1.

Malavieille, J., and Konstantinovskaya, E., 2010, Impact of surface processes on the growth of orogenic wedges: Insights from analog models and case studies: Geotectonics, v. 44, p. 541–558, https://doi.org/10.1134/S0016852110060075.

Malavieille, J., Lacassin, R., and Mattauer, M., 1984, Signification tectonique des lineations d'allongement dans les Alpes occidentales: Bulletin de la Société Géologique de France, v. S7-XXVI, p. 895–906, https://doi.org/10.2113/gssgfbull.S7-XXVI.5.895.

Matte, P., 2007, Variscan thrust nappes, detachments, and strike-slip faults in the French Massif Central: Interpretation of the lineations, *in* Hatcher Jr., R.D., Carlson, M.P., McBride, J.H., and Martínez Catalán, J.R., *eds*., 4–D Framework of Continental Crust: Geological Society of America Memoirs, v. 200, p. 391–402, https://doi.org/10.1130/2007.1200(20).

Matte, P., Lancelot, J., and Mattauer, M., 1998, La zone axiale hercynienne de la Montagne Noire n'est pas un "metamorphic core complex" extensif mais un anticlinal post-nappe à cœur anatectique: Geodinamica Acta, v. 11, p. 13–22, https://doi.org/10.1016/S0985-3111(98)80025-9.

Melezhik, V.A., Fallick, A.E., and Clark, T., 1997, Two billion year old isotopically heavy carbon: evidence from the Labrador Trough, Canada: Canadian Journal of Earth Sciences, v. 34, p. 271−285, https://www.doi.org/10.1139/e17-025.

Moorhead, J., and Hynes, A., 1990, Nappes in the internal zone of the northern Labrador Trough: Evidence for major early, NW-vergent basement transport: Geoscience Canada, v. 17, p. 241–244.

Perreault, S., and Hynes A., 1990, Tectonic evolution of the Kuujjuaq terrane, New Quebec Orogen: Geoscience Canada, v. 17, p. 238–240.

Pfiffner, O.A., 2017, Thick-skinned and thin-skinned tectonics: a global perspective: Geosciences, v. 7, 71, https://doi.org/10.3390/geosciences7030071.

Poirier, G.G., Perreault, S., and Hynes, A., 1990, Nature of the eastern boundary of the Labrador Trough near Kuujjuaq, Quebec: *in* Lewry, J.F., and Stauffer, M.R., *eds*., The Early Proterozoic Trans-Hudson Orogen of North America: Lithotectonic correlations and evolution: Geological Association of Canada, Special Paper 37, p. 397−412.

Rayner, N.M., Lafrance, I., Corrigan, D., and Charette, B., 2017, New U–Pb zircon ages of plutonic rocks from the Jeannin Lake area, Quebec: an evaluation of the Kuujjuaq domain and Rachel–Laporte Zone: Geological Survey of Canada, Current Research, 2017–4, 17 p.

Rohon, M.-L., Vialette, Y., Clark, T., Roger, G., Ohnenstetter, D., and Vidal., Ph., 1993, Aphebian mafic–ultramafic magmatism in the Labrador Trough (New

Quebec): its age and the nature of its mantle source: Canadian Journal of Earth Sciences, v. 30, p. 1582–1593, https://doi.org/10.1139/e93-136.

Rosenberg, C.L., Berger, A., Bellahsen, N., and Bousquet, R., 2015, Relating orogen width to shortening, erosion, and exhumation during Alpine collision: Tectonics, v. 34, p. 1306–1328, https://doi.org/10.1002/2014TC003736.

Selzer, C., Buiter, S.J.H., and Pfiffner, O.A., 2008, Numerical modeling of frontal and basal accretion at collisional margins: Tectonics, v. 27, TC3001, https://doi.org/10.1029/2007TC002169.

Simard, M., Lafrance, I., Hammouche, H., and Legouix, C., 2013, G.éologie de la région de Kuujjuaq et de la baie d'Ungava (SRNC 24J, 24K): Ministère de l'Énergie et des Ressources naturelles, Québec, RG 2013−04, 62 p.

Skulski, T., Wares, R.P., and Smith, A.D., 1993, Early Proterozoic (1.88–1.87 Ga) tholeiitic magmatism in the New Québec Orogen: Canadian Journal of Earth Sciences, v. 30, p. 1505–1520, https://doi.org/10.1139/e93-129.

Van Den Dreissche, J., and Brun, J.-P., 1989, Kinematic model of late Paleozoic extensional tectonics in the southern, French Massif Central: Comptes Rendus - Academie des Sciences, t. 309, Série II, p. 1607−1613.

Vanier, M.-A., Guilmette, C., Harris, L., Godet, A., Cleven, N., Charette, B., and Lafrance, I., 2017, Analyse structurale et microstructures des zones de cisaillement de la Rivière George et du Lac Tudor: Ministère de l'Énergie et des Ressources naturelles, Québec, MB 2017–12, 50 p.

Wardle, R.J., and Bailey, D.G., 1981, Early Proterozoic sequences in Labrador, *in* Campbell, F.H.A., *ed.*, Proterozoic basins of Canada: Geological Survey of Canada, Paper 81–10, p. 331–359, https://doi.org/10.4095/109385.

Wardle, R.J., Ryan, B., and Ermanovics, I., 1990, The eastern Churchill Province, Torngat and New Québec Orogens: An overview: Geoscience Canada, v. 17, p. 217–222.

Wardle, R.J., James, D.T., Scott, D.J., and Hall, J., 2002, The southeastern Churchill Province: synthesis of a Paleoproterozoic transpressional orogen: Canadian Journal of Earth Sciences, v. 39, p. 639–663, https://doi.org/10.1139/e02-004.

Wares, R.P., and Goutier, J., 1990, Deformational style in the foreland of the northern New Québec Orogen: Geoscience Canada, v. 17, p. 244–249.

Received November 2018
Accepted as revised February 2019

*For access to the Konstantinovskaya et al. (2019) supplementary files, (an enlarged version of Figure 3 and a Google Earth location map, .kmz format), please visit the GAC's open source GC Data Repository link for the Andrew Hynes Series: Tectonic Processes at: https://GAC.ca/GC-data-repository/.